Inorg. Chem. **2006**, *45*, 9985–10001

Forum

Insight into Heme Protein Redox Potential Control and Functional Aspects of Six-Coordinate Ligand-Sensing Heme Proteins from Studies of Synthetic Heme Peptides

Aaron B. Cowley,[†] Michelle L. Kennedy,[†] Svetlana Silchenko,[†] Gudrun S. Lukat-Rodgers,[‡] Kenton R. Rodgers,[‡] and David R. Benson*,[†]

Department of Chemistry, University of Kansas, Lawrence, Kansas 66045, and Department of Chemistry, North Dakota State University, Fargo, North Dakota 58105

Received December 28, 2005

We describe detailed studies of peptide-sandwiched mesohemes PSM^A and PSM^W, which comprise two histidine (His)-containing peptides covalently attached to the propionate groups of iron mesoporphyrin II. Some of the energy produced by ligation of the His side chains to Fe in the PSMs is invested in inducing helical conformations in the peptides. Replacing an alanine residue in each peptide of PSM^A with tryptophan (Trp) to give PSM^W generates additional energy via Trp side chain–porphyrin interactions, which enhances the peptide helicity and stability of the His-ligated state. The structural change strengthened His–Fe^{III} ligation to a greater extent than His–Fe^{II} ligation, leading to a 56-mV negative shift in the midpoint reduction potential at pH 8 ($E_{m,8}$ value). This is intriguing because converting PSM^A to PSM^W decreased heme solvent exposure, which would normally be expected to stabilize Fe^{II} relative to Fe^{III}. This and other results presented herein suggest that differences in stability may be at least as important as differences in porphyrin solvent exposure in governing redox potentials of heme protein variants having identical heme ligation motifs. Support for this possibility is provided by the results of studies from our laboratories comparing the microsomal and mitochondrial isoforms of mammalian cytochrome b_5. Our studies of the PSMs also revealed that reduction of Fe^{III} to Fe^{II} reversed the relative affinities of the first and second His ligands for Fe ($K_2^{III} > K_1^{III}$; $K_2^{II} < K_1^{II}$). We propose that this is a consequence of conformational mobility of the peptide components, coupled with the much greater ease with which Fe^{II} can be pulled from the mean plane of a porphyrin. An interesting consequence of this phenomenon, which we refer to as "dynamic strain", is that an exogenous ligand can compete with one of the His ligands in an Fe^{II}-PSM, a reaction accompanied by peptide helix unwinding. In this regard, the PSMs are better models of neuroglobin, CooA, and other six-coordinate ligand-sensing heme proteins than of stably bis(His)-ligated electron-transfer heme proteins such as cytochrome b_5. Exclusive binding of exogenous ligands by the Fe^{II} form of PSM^A led to positive shifts in its $E_{m,8}$ value, which increases with increasing ligand strength. The possible relevance of this observation to the function of six-coordinate ligand-sensing heme proteins is discussed.

Introduction

Research directed toward developing mimetic systems that reproduce structural features of heme proteins has a long and rich history.[1−7] Efforts in this area began well before the determination of the first heme protein crystal structures in the late 1960s,[8,9] when even the nature of heme ligation

* To whom correspondence should be addressed. E-mail: drb@ku.edu. Tel.: (785)864-4090. Fax: (785)864-5396.
[†] University of Kansas.
[‡] North Dakota State University.

(1) Wang, J. H. *Acc. Chem. Res.* **1970**, *3*, 90−97.
(2) Collman, J. P. *Acc. Chem. Res.* **1977**, *10*, 265−272.
(3) Traylor, T. G. *Acc. Chem. Res.* **1981**, *14*, 102−109.
(4) Baldwin, J. E.; Permutter, P. *Top. Curr. Chem.* **1984**, *121*, 181−220.
(5) Morgan, B.; Dolphin, D. *Struct. Bonding (Berlin)* **1987**, *64*, 115−201.
(6) Lombardi, A.; Nastri, F.; Pavone, V. *Chem. Rev.* **2001**, *101*, 3165−3189.
(7) Reedy, C. J.; Gibney, B. R. *Chem. Rev.* **2004**, *104*, 617−650.
(8) Nobbs, C. L.; Watson, H. C.; Kendrew, J. C. *Nature* **1966**, *209*, 339−341.
(9) Perutz, M. F.; Muirhead, H.; Cox, J. M.; Goaman, L. C. *Nature* **1968**, *219*, 131−139.

10.1021/ic052205k CCC: $33.50
Published on Web 12/04/2006

Chart 1. Structures of the Two Tautomers of His and His Analogues Used in Model Studies

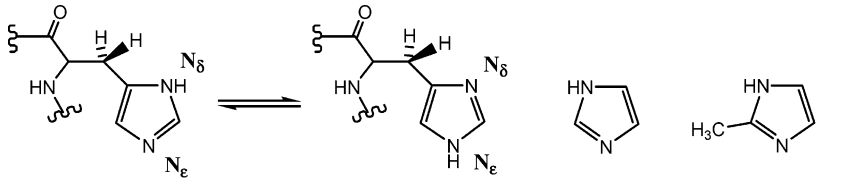

in known proteins was largely speculative.[10,11] Prior to the start of our studies in this area, there were relatively few reports of synthetic heme protein models containing peptide components of more than three amino acids.[12−20] In only three of those cases did the peptide components display biologically relevant conformations,[15,16,18,19] and only one[15,16] was soluble in water (the others were designed as membrane-penetrating ion channels). In each system, four[15,16,18] or eight[19] peptides had been covalently linked at symmetrical locations about the perimeter of a porphyrin. The covalent linkages fostered peptide−peptide interactions that led to the formation of one[15,16,18] or two[19] four-helix bundles oriented perpendicular to the porphyrin plane, an unknown motif in natural heme proteins.

Our goal was to create water-soluble heme protein mimetics exhibiting biologically relevant peptide conformations but which shared structural features with known heme proteins. At the beginning, our primary interest in heme protein design had a bioorganic focus, namely, learning to control peptide conformation.[21−27] We detected small but intriguing differences in the spectroscopic properties of the heme as the peptide sequence was varied, however, which kindled an interest in the bioinorganic chemistry of our systems. We have therefore de-emphasized design as a specific goal for the time being, to focus our efforts on carefully correlating heme properties with polypeptide structure in a small number of mimetics. Some of that work has already been published,[22,26,28−30] while some is reported herein for the first time. We feel that this approach has provided, and will continue to provide, fresh insight into the often subtle relationship between structure and function in natural heme proteins. One line of research described herein has shed light on possible factors important in the mechanisms of six-coordinate heme proteins that function as sensors of small molecules. We also expand upon previously published results[29] which suggested that differences in stability can outweigh differences in solvent exposure in tuning redox potentials of heme proteins sharing identical folds and ligation motifs.

Design Inspirations from the Protein Data Bank (PDB)

To identify common polypeptide structural motifs in heme binding pockets that could be incorporated into a model system, we performed a survey of heme protein crystal structures in the PDB.[31] The survey revealed a preponderance of α-helical secondary structure and a virtual absence of β structure above or below the heme plane. Proteins in which heme is surrounded partially or completely by β structure have since been discovered, as noted in a more recent and more thorough PDB survey performed by Reedy and Gibney.[7] Our PDB survey showed that the imidazolyl side chain of histidine (His) is the most common ligand to Fe in heme proteins and that His residues serving in this capacity are often located in or near helices spanning the heme. The His side chain has two tautomeric forms and, thus, both the N_δ and N_ϵ atoms can conceivably ligate to heme Fe (see Chart 1).[32] There were no proteins exhibiting His N_δ ligation at the time we performed our PDB survey, and only one has since been discovered.[33] These findings led to an initial goal of designing heme protein mimetics containing helical peptides spanning an iron porphyrin, with His residues within the helices ligating to Fe via their N_ϵ atoms.

Another commonality revealed in our PDB survey was extensive van der Waals contact between the large hydro-

(10) Keilin, J. *Nature* **1960**, *187*, 365−371.
(11) Harbury, H. A.; Cronin, J. R.; Fanger, M. W.; Hettinger, T. P.; Murphy, A. J.; Myer, Y. P.; Vinogradov, S. N. *Proc. Natl. Acad. Sci. U.S.A.* **1965**, *54*, 1658−1664.
(12) Momenteau, M.; Loock, B. *Biochim. Biophys. Acta* **1974**, *343*, 535−545.
(13) Molokoedov, A. S.; Filippovich, E. I.; Kazakova, N. A.; Evstigneeva, R. P. *Zh. Obshch. Khim. Ed. Engl.* **1977**, *47*, 1165−1172.
(14) Kazakova, N. A.; Radyukhin, V. A.; Luzgina, V. N.; Filippovich, E. I.; Kamyshan, N. V.; Kudryavtseva, E. V.; Evstigneeva, R. P. *Zh. Obshch. Khim. Ed. Engl.* **1983**, *52*, 1896−1906.
(15) Sasaki, T.; Kaiser, E. T. *J. Am. Chem. Soc.* **1989**, *111*, 380−381.
(16) Sasaki, T.; Kaiser, E. T. *Biopolymers* **1990**, *29*, 79−88.
(17) Casella, L.; Gullotti, M.; De Gioia, L.; Monzani, E.; Chillemi, F. *J. Chem. Soc., Dalton Trans.* **1991**, 2945−2953.
(18) Akerfeldt, K. S.; Kim, R. M.; Carmac, D.; Groves, J. T.; Lear, J. D.; DeGrado, W. F. *J. Am. Chem. Soc.* **1992**, *114*, 9656−9657.
(19) Mihara, H.; Nishino, N.; Hasegawa, R.; Fujimoto, T. *Chem. Lett.* **1992**, 1805−1808.
(20) Casella, L.; Gullotti, M.; De Gioia, L.; Bartesaghi, R.; Chillemi, F. *J. Chem. Soc., Dalton Trans.* **1993**, 2233−2239.
(21) Benson, D. R.; Hart, B. R.; Zhu, X.; Doughty, M. B. *J. Am. Chem. Soc.* **1995**, *117*, 8502−8510.
(22) Arnold, P. A.; Benson, D. R.; Brink, D. J.; Hendrich, M. P.; Jas, G. S.; Kennedy, M. L.; Petasis, D. T.; Wang, M. *Inorg. Chem.* **1997**, *36*, 5306−5315.
(23) Arnold, P. A.; Shelton, W. R.; Benson, D. R. *J. Am. Chem. Soc.* **1997**, *119*, 3181−3182.
(24) Wang, M.; Kennedy, M. L.; Hart, B. R.; Benson, D. R. *Chem. Commun.* **1997**, 883−884.
(25) Williamson, D. A.; Benson, D. R. *Chem. Commun.* **1998**, 961−962.
(26) Liu, D.; Williamson, D. A.; Kennedy, M. L.; Williams, T. D.; Morton, M. M.; Benson, D. R. *J. Am. Chem. Soc.* **1999**, *121*, 11798−11812.
(27) Liu, D.; Lee, K.-H.; Benson, D. R. *Chem. Commun.* **1999**, 1205−1206.
(28) Cowley, A. B.; Lukat-Rodgers, G. S.; Rodgers, K. R.; Benson, D. R. *Biochemistry* **2004**, *43*, 1656−1666.
(29) Kennedy, M. L.; Silchenko, S.; Houndonougbo, N.; Gibney, B. R.; Dutton, P. L.; Rodgers, K. R.; Benson, D. R. *J. Am. Chem. Soc.* **2001**, *123*, 4635−4636.
(30) Lee, K.-H.; Kennedy, M. L.; Buchalova, M.; Benson, D. R. *Tetrahedron* **2000**, *56*, 9725−9731.
(31) Berman, H. M.; Westbrook, J.; Feng, Z.; Gilliland, G.; Bhat, T. N.; Weissig, H.; Shindyalov, I. N.; Bourne, P. E. *Nucleic Acids Res.* **2000**, *28*, 235−242.
(32) Chakrabarti, P. *Protein Eng.* **1990**, *4*, 57−63.
(33) Iverson, T. M.; Arciero, D. M.; Hsu, B. T.; Logan, M. S. P.; Hooper, A. B.; Rees, D. C. *Nat. Struct. Biol.* **1998**, *5*, 1005−1012.

Scheme 1. Stepwise Equilibrium Constants for Binding of ImH by an Iron(II) or Iron(III) Porphyrin (Porphyrin Represented in a Planar Fashion)[a]

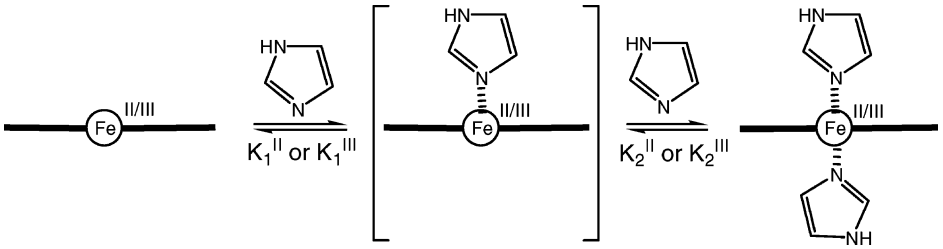

[a] The five-coordinate mono(ImH) complex is not observed.

phobic porphyrin moiety and apolar amino acid side chains in its binding pocket. We were intrigued to observe at least one aromatic side chain engaging in an edge-to-face (T-stacking) or face-to-face (π-stacking) interaction with the porphyrin in each heme protein structure in the PDB.[25,26] Information from other databases indicated some variability with respect to the identity of the aromatic side chain but that the interactions were invariant. This caught our attention as a potentially useful design feature because evidence available at the time suggested that interactions between aromatic groups were stronger and more specific than dispersion interactions between aliphatic groups.[34,35]

Other Design Considerations

Previous Studies of His-Ligated Heme Protein Mimetics. The earliest heme protein mimetics, and the simplest in terms of structure, were complexes between heme or another iron porphyrin and ligands such as imidazole (ImH; Chart 1) representing the His side chain.[36,37] Such complexes continue to provide insight into the relationship between structure and function in His-ligated heme proteins.[38,39] Insofar as the design of heme protein mimetics having biologically relevant peptide conformations is concerned, such complexes pose two major challenges. First, excess ImH is required to achieve saturation binding, particularly in water and other polar solvents that compete as ligands to Fe. Second, the equilibrium constant for binding of a second 1 equiv of ImH to an iron(II) or iron(III) porphyrin is about 1 order of magnitude larger than that for binding of the first ImH ($K_2^{III} > K_1^{III}$ and $K_2^{II} > K_1^{II}$; Scheme 1)[40,41] because binding of the second ligand converts iron from the high-spin state to the low-spin state. The preference of ferric and ferrous porphyrins for bis(ImH) ligation may not be a problem if one's goal is to develop models of low-spin bis-(His)-ligated heme proteins such as cytochrome b_5 (cyt b_5). It does, however, prevent recapitulation of the high-spin mono(His) ligation exhibited by myoglobin (Mb), hemoglobin (Hb), and other heme proteins of interest to designers.

A very general solution for avoiding bis(ImH) ligation by an iron porphyrin, and for obviating the need for excess ligand in either mono(His)- or bis(His)-ligated heme protein mimetics, is to use covalent linkers (for reviews of early efforts, see refs 3 and 5). Metalloporphyrins with one or two covalently appended ligands, sometimes referred to as "tailed" porphyrins, take advantage of a phenomenon known as the chelate effect. Simply put, a well-designed linker lowers the entropy of ligation for an intramolecular ligand relative to the analogous exogenous ligand, and the intramolecular ligand therefore binds more strongly. The first tailed porphyrins, reported by Lautsch and co-workers in 1958, comprised two identical His-containing tripeptides linked to the propionate groups of mesoheme via their N termini.[42] Mesoheme (iron mesoporphyrin IX; FeMPIX) is a readily available heme derivative in which the chemically reactive vinyl groups of heme (iron protoporphyrin IX; FePPIX) are replaced by ethyl groups. Subsequent studies in other groups focused on optimizing the His−Fe ligation strength in peptide−iron porphyrin adducts by varying the location of His within the peptide sequence,[43,44] while some researchers tackled the greater synthetic challenge of linking a single His-containing peptide to an iron porphyrin.[13,45−47]

Chang and Traylor concluded that His-containing peptides were inadequate for obtaining optimally stable His−Fe bonds, so in developing the first functional model of the Mb active site, they attached ImH to the propionate group of a heme derivative via a three-C aliphatic chain.[48] Switching from a peptide linker to a synthetic linker in this "chelated heme" further aided its utility as a Mb model by conferring solubility in relatively nonpolar organic solvents. This provided a local heme dielectric environment similar to that in Mb, thereby allowing reversible O_2 binding at cryogenic temperatures.[49] At higher temperatures and in more polar

(34) Hunter, C. A.; Sanders, J. K. M. *J. Am. Chem. Soc.* **1990**, *112*, 5525−5534.
(35) Jorgensen, W. L.; Severance, D. L. *J. Am. Chem. Soc.* **1990**, *112*, 4768−4774.
(36) Corwin, A. H.; Bruck, S. D. *J. Am. Chem. Soc.* **1958**, *80*, 4736−4739.
(37) Corwin, A. H.; Erdman, J. G. *J. Am. Chem. Soc.* **1946**, *68*, 2473−2478.
(38) Walker, F. A. *Chem. Rev.* **2004**, *104*, 589−615.
(39) Hu, C.; Roth, A.; Ellison, M. K.; An, J.; Ellis, C. M.; Schulz, C. E.; Scheidt, W. R. *J. Am. Chem. Soc.* **2005**, *127*, 5675−5688.
(40) Nesset, M. J. M.; Shokhirev, N. V.; Enemark, P. D.; Jacobson, S. E.; Walker, F. A. *Inorg. Chem.* **1996**, *35*, 5188−5200.
(41) Safo, M. K.; Nesset, M. J. M.; Walker, F. A.; Debrunner, P. G.; Scheidt, W. R. *J. Am. Chem. Soc.* **1997**, *119*, 9438−9448.
(42) Lautsch, V. W.; Wiemer, B.; Zschenderlein, P.; Kraege, H. J.; Bandel, W.; Gunther, D.; Schulz, G.; Gnichtel, H. *Kolloid Z.* **1958**, *161*, 36−49.
(43) Losse, G.; Mueller, G. *Hoppe−Seyler's Z. Physiol. Chem.* **1962**, *327*, 205−16.
(44) Van der Heijden, A.; Peer, H. G.; Van den Oord, A. H. A. *J. Chem. Soc., Chem. Commun.* **1971**, 369−370.
(45) Castro, C. E. *Bioinorg. Chem.* **1974**, *4*, 45−65.
(46) Warme, P. K.; Hager, L. P. *Biochemistry* **1970**, *9*, 1606−1614.
(47) Momenteau, M.; Rougee, M.; Loock, B. *Eur. J. Biochem.* **1976**, *71*, 63−76.
(48) Chang, C. K.; Traylor, T. G. *Proc. Natl. Acad. Sci. U.S.A.* **1973**, *70*, 2647−2650.
(49) Chang, C. K.; Traylor, T. G. *J. Am. Chem. Soc.* **1973**, *95*, 5810−5811.

environments, autoxidation would occur to give initially a ferric porphyrin and superoxide and eventually a μ-oxo ferric porphyrin dimer. The role of a low dielectric medium in achieving reversible O_2 binding can be understood by considering that heme and other porphyrins are dibasic ligands. Ferric porphyrins therefore bear a formal 1+ charge on Fe, while Fe in ferrous porphyrins is uncharged. As a result, Fe^{II} is stabilized relative to Fe^{III} as the solvent polarity decreases (the $Fe^{III/II}$ redox couple becomes more positive). Chang and Traylor's achievement probably contributed to a subsequent decline in the literature reports of heme protein mimetics containing peptidic components, which tend to only be soluble in polar solvents.

Challenge of Inducing Helical Conformations in Peptides. Peptides tend to adopt unstructured (random-coil) conformations in aqueous solution, even if the corresponding sequence in a protein is helical.[50] The main factor discouraging a random-coil peptide from becoming helical is the entropically unfavorable decrease in conformational freedom of the peptide backbone and of many amino acid side chains (particularly aromatic amino acids and residues with β branches[51,52]). In proteins, this is compensated for by (1) long-range interactions between amino acid side chains in the helix and those in other units of secondary structure (salt bridges, hydrogen bonds, dispersion forces, etc.) and (2) the entropically favorable shedding of high-energy water molecules solvating apolar moieties, better known as the hydrophobic effect.[53−55] It was demonstrated that alanine (Ala) is the naturally occurring amino acid with the greatest tolerance for residing in an α helix[51,52,56] and that Ala-based peptides having evenly spaced glutamate (Glu) or lysine (Lys) residues for water solubility formed stable helices as long as they contained at least 16 residues (4.4 helical turns).[56] Helical conformations could be induced in peptides of shorter length or more diverse sequence if, for example, covalent bonds[57−59] or a sufficient number of ionic interactions[60] were formed between appropriately spaced amino acid side chains. We were particularly intrigued by two reports showing helix induction via transition-metal ion coordination by a pair of amino acid side chains.[61,62] These reports led us to surmise that it should be possible to achieve helix induction via His−Fe ligation in a covalent peptide−iron porphyrin adduct. The general strategy in the case of bis(His) ligation is shown in Scheme 2.

Scheme 2. Helix Induction in a Peptide-Sandwiched Mesoheme (PSM)[a]

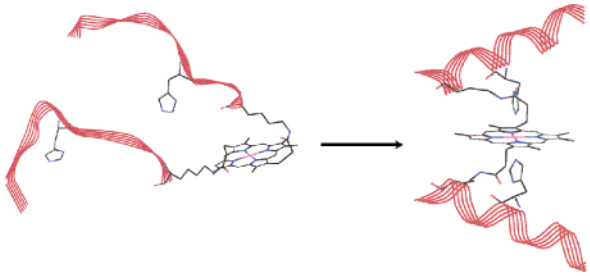

[a] The His-ligated structure is our computer-generated model of PSM^A built from MPII.

Biological Relevance of Heme Protein Mimetics Exhibiting Helix Induction

The multiple interactions between heme and the polypeptide, together with the hydrophobic effect, endow heme proteins with high thermodynamic stability.[53] These factors also play major roles in stabilizing the polypeptide conformation in the heme binding pocket, as exemplified by the soluble heme binding domain of cyt b_5, which comprises two hydrophobic cores separated by a five-stranded β sheet (structure on the right in Scheme 3).[63] The bis(His)-ligated heme is surrounded by a four-helix bundle in core 1, with the β sheet forming the base of the heme binding pocket. When heme is absent from core 1, the polypeptide defining the four-helix bundle is almost completely disordered (structure on the left in Scheme 3) but core 2 and most of the β sheet adopt a holo-like fold.[64,65] Heme binding by apocytochrome b_5 (apo-b_5) induces and stabilizes local polypeptide conformation (Scheme 3). Heme protein mimetics in which His−Fe coordination induces a helical structure therefore have the potential to shed light on factors important in thermodynamic and conformational stability of His-ligated heme proteins and on how differences in the stability and structure might affect functional properties.

Design Targets

Peptide-Sandwiched Mesohemes. The bis(peptide)−iron porphyrin adduct represented in Scheme 2 is the most successful of our initial design targets, which we dubbed peptide-sandwiched mesohemes (PSMs; see also Chart 2). The first example was reported in 1995.[21] An important aim in the initial "proof of principle" stage was to avoid reactivity problems and synthetic and purification challenges. Thus, like others before us, we chose (1) to use MPIX because it was commercially available and allowed us to avoid the reactive vinyl groups of PPIX and (2) to attach two identical His-containing peptides to the MPIX propionate groups. We

(50) Scholtz, J. M.; Baldwin, R. L. *Annu. Rev. Biophys. Biomol. Struct.* **1992**, *21*, 95−118.
(51) Padmanabhan, S.; Marqusee, S.; Ridgeway, T.; Laue, T. M.; Baldwin, R. L. *Nature* **1990**, *344*, 268−270.
(52) Merutka, G.; Lipton, W.; Shalongo, W.; Park, S. H.; Stellwagen, E. *Biochemistry* **1990**, *29*, 7511−7515.
(53) Hargrove, M. S.; Olson, J. S. *Biochemistry* **1996**, *35*, 11310−11318.
(54) Makhatadze, G. I.; Privalov, P. L. *Adv. Protein Chem.* **1995**, *47*.
(55) Dill, K. A. *Biochemistry* **1990**, *29*, 7133−7155.
(56) Marqusee, S.; Robbins, V. H.; Baldwin, R. L. *Proc. Natl. Acad. Sci. U.S.A.* **1989**, *86*, 5286−5290.
(57) Jackson, D. Y.; King, D. S.; Chmielewski, J.; Singh, S.; Schultz, P. G. *J. Am. Chem. Soc.* **1991**, *113*, 9391−9392.
(58) Chorev, M.; Roubini, E.; McKee, R. L.; Gibbons, S. W.; Goldman, M. E.; Caulfield, M. P.; Rosenblatt, M. *Biochemistry* **1991**, *30*, 5968−5974.
(59) Osapay, G.; Taylor, J. W. *J. Am. Chem. Soc.* **1992**, *114*, 6966−6973.
(60) Lyu, P. C.; Gans, P. J.; Kallenbach, N. R. *J. Mol. Biol.* **1992**, *223*, 343−350.
(61) Ghadiri, M. R.; Choi, C. *J. Am. Chem. Soc.* **1990**, *112*, 1630−1632.
(62) Ruan, F.; Chen, Y.; Hopkins, P. B. *J. Am. Chem. Soc.* **1990**, *112*, 9403−9404.
(63) Durley, R. C. E.; Mathews, F. S. *Acta Crystallogr.* **1996**, *D52*, 65−76.
(64) Falzone, C. J.; Mayer, M. R.; Whiteman, E. L.; Moore, C. D.; Lecomte, J. T. J. *Biochemistry* **1996**, *35*, 6519−6526.
(65) Falzone, C. J.; Wang, Y.; Vu, B. C.; Scott, N. L.; Bhattacharya, S.; Lecomte, J. T. J. *Biochemistry* **2001**, *40*, 4879−4891.

Scheme 3. Binding of Heme by Apocytochrome b_5 (PDB 1i8c),[65] Which Stabilizes the Polypeptide Structure in the Holoprotein (PDB 1CYO)[63]

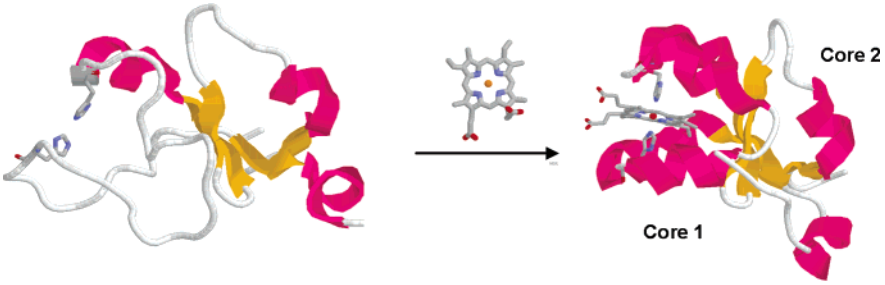

Chart 2. Structures of the PSMs and mPSM Used in Most of the Studies Described Herein[a]

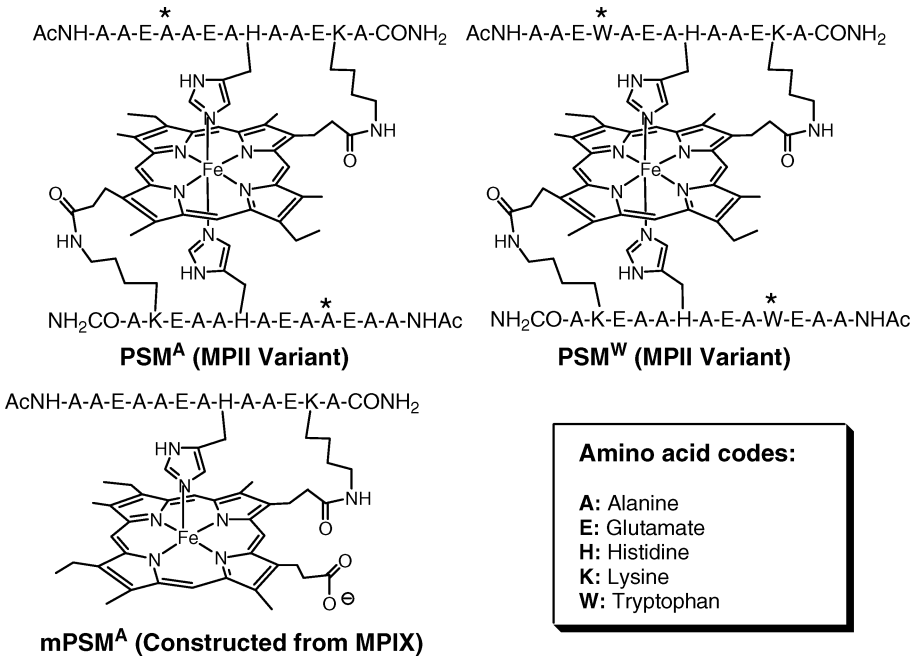

[a] The residues that differ in PSM^A and PSM^W are indicated with asterisks. Also shown are the amino acids corresponding to the one-letter codes used in the structures.

felt that this would be more convenient than attaching a single peptide to FeMPIX, which would afford a statistical mixture of products and, thus, a lower yield of the desired product.

Monopeptide Analogues of the PSMs. Despite the potential for purification problems and the reality of diminished yields, we were interested in the monopeptide analogues of the PSMs (mPSMs; Chart 2) as models of mono(His)-ligated heme proteins. The mPSMs were always present as side products in PSM preparations and were thus collected and at least partially characterized, but only recently have they become a central focus of our studies.[28] The mPSMs were the first synthetic, covalent, mono(ImH)-ligated heme peptides exhibiting high solubility in water and other polar protic solvents to be reported. The only other heme peptides exhibiting this characteristic are proteolytic fragments of cytochrome *c*.[66]

Design Round I: Optimizing Peptide Helicity

Our computer-aided design efforts indicated that inducing peptide helicity would be better achieved by attaching His-containing peptides to the propionate groups of FeMPIX via the ϵ-amino groups of Lys residues rather than by their N termini, as had been done by Lautsch[42] and others.[13,14,43,44] We opted to use a peptide containing 13 amino acids (3.6 helical turns), sufficiently long to span the entire "face" of a porphyrin but three residues shorter than is known to allow stable helix formation in Ala-based peptides.[56] Combined with the presence of a "helix-breaking" His residue near the peptide center, this virtually guaranteed a random-coil conformation in the His-dissociated form of a PSM. To endow the PSMs with solubility in water at neutral pH, we incorporated three glutamic acid (Glu) residues into each peptide at positions from which their side chains would extend into the solvent. An additional part of our design strategy was to "cap" the peptide N and C termini as amides, which among other advantages renders them more like helical segments in proteins.

Our computer-aided design approach[21,22] identified only three Lys−His separations that would be compatible with helix induction in a PSM: $i, i + 4$; $i, i - 4$; $i, i - 3$. We focus herein on the one with $i, i - 4$ Lys−His spacing

(66) Adams, P. A.; Baldwin, D. A.; Marques, H. M. In *Cytochrome c. A Multidisciplinary Approach*; Scott, R. A., Mauk, A. G., Eds.; University Science Books: Sausalito, CA, 1996; Vol.xd5 p∧pp Chapter 20.

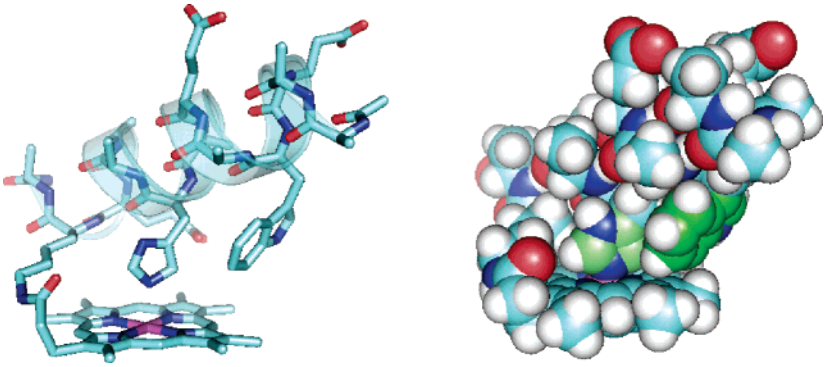

Figure 1. Energy-minimized partial structure of PSM^W obtained in our modeling studies,[25,26] highlighting the possibility for edge-to-face interactions between a Trp residue at position 4 and the porphyrin. H atoms have been omitted from the structure on the left for reasons of clarity. To aid in visualizing the space-filling representation on the right, the C atoms in the His ligand and the Trp side chain have been colored lime and green, repectively.

(referred to hereafter as PSM^A; see Chart 2), which was shown by circular dichroism (CD) spectroscopy to exhibit the highest helix content (~50%) in aqueous solution at pH 7 and 8 °C (the lowest temperature accessible on the instrument available to us at the time; a low temperature was used to maximize the helix content).[22] A desirable feature of PSM^A in terms of design was the fact that only a single combination of His side-chain torsional angles appeared to be compatible with helix induction. With this combination, the helix axes in PSM^A would be angled ~30° relative to the porphyrin plane, placing the peptide C termini (near the covalent Lys−propionate linkage) in van der Waals contact with the porphyrin (see Scheme 2). These design predictions were confirmed in a nuclear magnetic resonance (NMR) study of the mesoporphyrin II (MPII) variant of PSM^A (vide infra), in which Fe was replaced by Co^{III} to give an air-stable diamagnetic complex.[26]

It is important to emphasize that (1) the peptide used in constructing the PSMs exhibited random-coil conformations in aqueous solution, (2) the PSMs displayed bis(His) ligation at neutral pH, as demonstrated initially by UV/vis spectroscopy, and (3) we observed no significant difference in the helix content between any PSM and the corresponding mPSM, indicating mono(His) ligation in the latter.[21,22] Mono(His) ligation in the mPSMs is also supported by various spectroscopic indicators discussed in a later section.

Diastereomer Problem. The only symmetry element in MPIX is the porphyrin plane, but the two propionate groups are related by a pseudo-C_2 rotation axis. Hence, the two peptides in the bis(His)-ligated form of a PSM built from FeMPIX should be related by a 2-fold rotation axis (assuming no restrictions on His ligand orientation). Two diasteromeric bis(His)-ligated complexes are possible, however, interchangeable when the His ligands dissociate and trade places.[21] Once we had achieved proof of principle with the PSMs described above, we desired to avoid this "diastereomer problem". One successful approach was to incorporate protein-like design features into a PSM that strongly stabilized one diastereomer relative to the other.[27] A much more general strategy was to replace MPIX with MPII, a synthetic analogue having C_{2h} symmetry.[24,26] The two peptides in a PSM built from FeMPII are not related by symmetry. Thus, when the His ligands dissociate from Fe and trade places, the peptides will swap structural properties and orientations relative to the porphyrin. As long as the two peptides have the same sequence, the exchange process will not alter the overall molecular architecture. Chart 2 shows the variant of PSM^A constructed from MPII, and all results reported in this paper refer to this variant. It should be noted that the mPSMs can exist in two diastereomeric forms regardless of whether they are built from MPIX or MPII. For reasons of economy, we therefore utilized FeMPIX when synthesizing the mPSMs (see Chart 2).

Design Round 2: Introduction of Aromatic Side Chain−Porphyrin Interactions

The goal in our second round of design was to introduce aromatic amino acid side chain−porphyrin interactions into PSM^A with the hope of enhancing the helix content. In our computer model of PSM^A with fully helical peptides (Scheme 2),[22] Ala-4 in each peptide (located four residues away from the His ligand, toward the N terminus) was poised above the porphyrin. Replacing Ala-4 with Trp in silico indicated that the Trp side chain could readily engage in edge-to-face interactions with the porphyrin[25,26] (Figure 1). The corresponding phenylalanine (Phe) replacement indicated that the Phe side chain was too short to contact the porphyrin. These design predictions have been verified experimentally,[26] but for purposes of brevity, we will limit our discussion to the PSM^A "mutant" in which the two Ala-4 residues have been replaced by Trp (hereafter PSM^W). Converting PSM^A to PSM^W increased the helix content from ~50% to ~83% in aqueous solution at 8 °C, as determined by CD, an effect confirmed by an increase in the intrapeptide nuclear Overhauser effect (NOE) signal intensity in the 2D NOESY spectrum of Co^{III}-PSM^W relative to that of Co^{III}-PSM^A.[26] The strongest evidence indicating that the Trp side chain−porphyrin interactions in PSM^W were responsible for the enhanced helix content relative to PSM^A was provided in NMR studies of diamagnetic Co^{III}-PSM^W.[26] The aromatic side-chain protons were shifted strongly upfield relative to their positions in the monomeric peptide, indicating a location in the shielding region of the porphyrin (i.e., with the C−H bonds directed toward the porphyrin π system). Furthermore, the chemical shift pattern of the Trp side chain in PSM^W

matched expectations for its geometry relative to the porphyrin predicted in our computer-aided design studies.

While pursuing the NMR studies described in previous sections aimed at comparing the Co^{III} derivatives of PSM^A and PSM^W, we developed an alternative strategy for verifying that the Trp incorporation had significantly increased the peptide helix content: H−D exchange (HDX) reactions monitored by electrospray ionization mass spectrometry.[26] Increasing the peptide helix content diminishes exposure of the peptide backbone amides to water,[67] which was known to slow the reaction between the NH groups and D_2O to give ND groups.[68] HDX reactions were initiated by rapidly diluting an aliquot of a concentrated dimethyl sulfoxide (DMSO) solution of Fe^{III}-PSM into the deuterated buffer solution. The solutions were then slowly infused into the mass spectrometer, and the time-dependent increase in the average mass was monitored. Our results showed that exchange was complete within 5 min for PSM^A, but the average rate was more than 100-fold slower than that reported in the literature for a simple peptide of similar length and helix content (results were adjusted for differences in the solution pH).[69] This suggested that the two-point peptide−porphyrin attachment in the PSM places severe restrictions on peptide conformational mobility. Exchange in PSM^W was dramatically slower than that in PSM^A, with more than eight NH's in PSM^W exhibiting half-lives for the reaction of >9 min.

Comparison between the PSMs and Mimochromes

In 1997, Pavone and co-workers reported Mimochrome I,[70,71] which bore a striking resemblance to the PSMs. Mimochrome I comprised two identical nine-residue helical peptides attached to the propionate groups of a heme derivative (iron deuteroporphyrin IX; FeDPIX) via the side chains of Lys residues, with the side chain of a His residue in each peptide ligating to Fe (*i*, *i* − 3 Lys−His spacing). Mimochrome I and its subsequently reported variants also share with the PSMs the possibility for two diastereomeric forms,[72] one of which could be made dominant by the application of careful design principles.[73] Pavone and co-workers also utilized Co^{III} rather than Fe^{III} as the central metal in the mimochromes as an approach for solving the diastereomer problem.[74] Use of Co^{III} rendered the two isomers inert to ligand exchange, allowing them to be separated and structurally characterized, first by NMR[74] and more recently by X-ray crystallography.[75] The most important distinctions between the mimochromes and the PSMs relate to design: (1) mimochrome design was inspired by the structure of a specific heme protein, hemoglobin, and (2) His−Fe interactions in the mimochromes were ascribed no special role in the peptide conformational properties.

Other His-Ligated, Helical Heme Protein Mimetics

Bis(peptide)−Porphyrin Complexes. In 1998, Suslick and co-workers reported helix induction in reversible 2:1 complexes between amphiphilic His-containing peptides and a water-soluble iron porphyrin, thereby demonstrating that covalent peptide−porphyrin bonds are not essential for achieving helix induction in a bis(His)-ligated heme protein mimetic.[76] We came to the same conclusion in studies with analogues of the PSMs in which the peptide−porphyrin linkers were replaced by a peptide−peptide disulfide bridge.[23] Reaction between the randomly configured peptide dimer and cobalt(III) octaethylporphyrin yielded an exchange-inert, bis(His)-ligated complex exhibiting helix induction similar to that displayed by PSM^A. Suslick[77] and Mihara[78] subsequently reported similar complexes between bis(His) "hairpin peptides" and iron porphyrins but with the uncomplexed peptide dimers already exhibiting some helix content due to hydrophobic interactions between the amino acid side chains in the two peptides. Suslick's group recently took this idea one step further, forming complexes between iron(III) or cobalt(III) porphyrins and His-containing peptides that had been linked together at both termini to form macrocycles.[77,79] The cyclic peptides bound iron porphyrins up to 10^6 times more strongly than His itself.

Maquettes and Related Heme-Binding Four-Helix Bundles. After the start of our design studies but prior to publication of our first results, the Dutton and DeGrado groups reported preformed four-helix-bundle assemblies that bound either one[80] or four[81] hemes reversibly and with sufficient strength that a significant excess of heme was not required. Many variations on these heme protein "maquettes" have subsequently been reported,[7,82−85] including examples in which bundle formation is initiated by the peptide−heme interactions.[86] In addition to demonstrating the power of

(67) Englander, S. W.; Kallenbach, N. R. *Q. Rev. Biophys.* **1983**, *16*, 521−655.
(68) Wagner, D. S.; Melton, J. G.; Yan, Y.; Erickson, B. W.; Anderegg, R. J. *Protein Sci.* **1994**, *3*, 1305−1314.
(69) Stevenson, C. L.; Anderegg, R. J.; Borchardt, R. T. *J. Am. Soc. Mass Spectrom.* **1993**, *4*, 646−651.
(70) Nastri, F.; Lombardi, A.; Morelli, G.; Maglio, O.; D'Auria, G.; Pedone, C.; Pavone, V. *Chem.—Eur. J.* **1997**, *3*, 340−349.
(71) Lombardi, A.; Nastri, F.; Sanseverino, M.; Maglio, O.; Pedone, C.; Pavone, V. *Inorg. Chim. Acta* **1998**, *275*−*276*, 301−313.
(72) Fatturosso, R.; De Pasquale, C.; Morelli, G.; Pedone, C. *Inorg. Chim. Acta* **1998**, *278*, 76−82.
(73) Lombardi, A.; Nastri, F.; Marasco, D.; Maglio, O.; De Sanctis, G.; Sinibaldi, F.; Santucci, R.; Coletta, M.; Pavone, V. *Chem.—Eur. J.* **2003**, *9*, 5643−5654.
(74) D'Auria, G.; Maglio, O.; Nastri, F.; Lombardi, A.; Mazzeo, M.; Morelli, G.; Paolillo, L.; Pedone, C.; Pavone, V. *Chem.—Eur. J.* **1997**, *3*, 350−362.
(75) Costanzo, L.; Geremia, S.; Randaccio, L.; Nastri, F.; Maglio, O.; Lombardi, A.; Pavone, V. *J. Biol. Inorg. Chem.* **2004**, *9*, 1017−1027.
(76) Huffman, D. L.; Rosenblatt, M. M.; Suslick, K. S. *J. Am. Chem. Soc.* **1998**, *120*, 6183−6184.
(77) Rosenblatt, M. M.; Huffman, D. L.; Wang, X.; Remmer, H. A.; Suslick, K. S. *J. Am. Chem. Soc.* **2002**, *124*, 12394−12395.
(78) Sakamoto, S.; Obataya, I.; Ueno, A.; Mihara, H. *J. Chem. Soc., Perkin Trans. 2* **1999**, 2059−2069.
(79) Rosenblatt, M. M.; Wang, J.; Suslick, K. S. *Proc. Natl. Acad. Sci. U.S.A.* **2003**, *100*, 13140−13145.
(80) Choma, C. T.; Lear, J. D.; Nelson, M. J.; Dutton, P. L.; Roberson, D. E.; DeGrado, W. F. *J. Am. Chem. Soc.* **1994**, *116*, 856−865.
(81) Robertson, D. E.; Farid, R. S.; Moser, C. C.; Urbauer, J. L.; Mulholland, S. E.; Pidikiti, R.; Lear, J. D.; Wand, A. J.; DeGrado, W. F.; Dutton, P. L. *Nature* **1994**, *368*, 425.
(82) Gibney, B. R.; Dutton, P. L. *Adv. Inorg. Chem.* **2001**, *51*, 409−455.
(83) Rau, H. K.; DeJonge, N.; Haehnel, W. *Angew. Chem., Int. Ed.* **2000**, *39*, 250−253.
(84) Rau, H. K.; Haehnel, W. *J. Am. Chem. Soc.* **1998**, *120*, 468−476.
(85) Xu, Z.; Farid, R. S. *Protein Sci.* **2001**, *10*, 236−249.

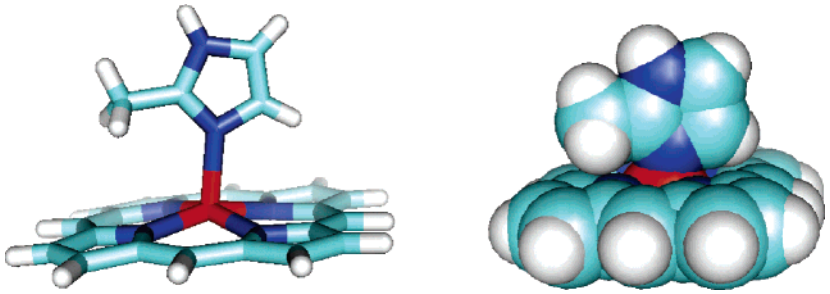

Figure 2. X-ray crystal structure of the complex between 2-MeImH and tetraphenylporphyrin[95] (phenyl rings removed for clarity) highlighting the out-of-plane displacement of Fe^{II} due to face strain.

computerized protocols for designing heme proteins with nativelike structure,[86,87] work with the maquettes and related species has provided tremendous insight into control of the redox potential in bis(His)-ligated mono- and multiheme proteins.[88−90] Heme-binding helical bundles also have potential applications in biotechnology, as exemplified in research by Haehnel and co-workers.[91]

Some very recent work with maquettes has demonstrated the utility of unnatural amino acids[92,93] and unnatural porphyrins[87] for extending the range of structural and functional properties that can be accessed in heme−polypeptide assemblies. We highlight one recent report that has relevance to studies from our laboratories described herein, in which Gibney and co-workers described the first reversible heme−polypeptide complex exhibiting mono(ImH)−Fe^{II} ligation.[93] This was achieved by replacing the His ligand in a monoheme four-helix-bundle maquette with an unnatural analogue containing a methyl group adjacent to the ligating N atom, an approach inspired by a seminal 1973 report by Collman and Reed showing that 2-methylimidazole (2-MeImH; Chart 1) formed a 1:1 complex with an iron(II) porphyrin (Figure 2).[94] Potential steric interactions between the methyl group and the porphyrin are relieved if Fe^{II} moves out of the mean porphyrin plane,[95] which virtually abolishes affinity for a second 1 equiv of 2-MeImH[94,96−98] and also weakens binding of Hb's natural ligand O_2.[99] Collman and co-workers therefore touted[99] this five-coordinate complex as a model for the tense state of hemoglobin (T-Hb), in which Fe^{II} is also pulled substantially out of the heme plane.[9] Ligation of His ligands to heme Fe via N_δ would achieve the same effect, providing a reasonable explanation for the near absence of this motif in natural heme proteins.

Probing Heme Ligation in the Fe^{III}-PSMs

We have employed a variety of spectroscopic methods to examine heme ligation in the PSMs and mPSMs. Useful benchmarks in spectroscopic studies of the PSMs have been the bis(ImH) complexes of FeMPIX [FeMPIX$(ImH)_2$] and FePPIX [FePPIX$(ImH)_2$]. Insight into mPSM ligation properties has largely been provided by comparing their spectroscopic characteristics with those reported for mono(His)-ligated heme proteins and mono(ImH)-ligated heme protein mimetics. In the following sections, we focus on PSM^A and the corresponding monopeptide system ($mPSM^A$), which have served as the basis for most of the work described herein. Unless otherwise noted, studies were performed at 25 °C and pH 7 in aqueous solution.

UV/vis Spectroscopy. The UV/vis spectrum of PSM^A exhibits a Soret band with $\lambda_{max} = 402$ nm, a β (Q_v) band at 525 nm, and an α (Q_o) band at 565 nm[21] (Figure S1A in the Supporting Information), indicative of low-spin bis(His)-ligated Fe^{III}. UV/vis spectra of mPSMs are indicative of high-spin ($S = {}^5/_2$) Fe^{III} and display a strong concentration dependence due to aggregation, which could be abolished by the use of methanol as a cosolvent.[21,22] The UV/vis spectrum of Fe^{III}-$mPSM^A$ in aqueous solution containing 40% (v/v) MeOH (Figure S1B in the Supporting Information) exhibits Soret band λ_{max} at 391 nm, a broad band centered at 491 nm, and a ligand-to-metal charge-transfer band at 620 nm.[28]

Resonance Raman (RR) Spectroscopy. RR spectra of PSM^A [29] and $mPSM^A$,[28] obtained using excitation at 406.7 nm, are compared in Figure S2 in the Supporting Information. The PSM^A spectrum features a spin-state marker band (ν_3) at 1507 cm^{-1} and an oxidation-state marker band (ν_4) centered at 1376 cm^{-1}. The corresponding bands in RR spectra of Fe^{III}-MPIX$(ImH)_2$ ($\nu_3 = 1505$ cm^{-1}; $\nu_4 = 1375$ cm^{-1})[100,101] and ferric cyt b_5 ($\nu_3 = 1506$ cm^{-1}; $\nu_4 = 1374$ cm^{-1})[102] occur at nearly identical frequencies. The RR spectra of PSM^A and PSM^W are virtually identical (Figure S3 in the

(86) Ghirlanda, G.; Osyczka, A.; Liu, W.; Antolovich, M.; Smith, K. M.; Dutton, P. L.; Wand, A. J.; DeGrado, W. F. *J. Am. Chem. Soc.* **2004**, *126*, 8141−8147.
(87) Cochran, F. V.; Wu, S. P.; Wang, W.; Nanda, V.; Saven, J. G.; Therien, M. J.; DeGrado, W. F. *J. Am. Chem. Soc.* **2005**, *127*, 1346−1347.
(88) Gibney, B. R.; Rabanal, F.; Reddy, K. S.; Dutton, P. L. *Biochemistry* **1998**, *37*, 4635−4643.
(89) Shifman, J. M.; Gibney, B. R.; Sharp, R. E.; Dutton, P. L. *Biochemistry* **2000**, *39*, 14813−14821.
(90) Gibney, B. R.; Huang, S. S.; Skalicky, J. J.; Fuentes, E. J.; Wand, A. J.; Dutton, P. L. *Biochemistry* **2001**, *40*, 10550−10561.
(91) Willner, I.; Heleg-Shabtai, V.; Katz, E.; Rau, H. K.; Haehnel, W. *J. Am. Chem. Soc.* **1999**, *121*, 6455−6468.
(92) Privett, H. K.; Reedy, C. J.; Kennedy, M. L.; Gibney, B. R. *J. Am. Chem. Soc.* **2002**, *124*, 6828−6829.
(93) Zhuang, J.; Amoroso, J. H.; Kinloch, R.; Dawson, J. H.; Baldwin, M. J.; Gibney, B. R. *Inorg. Chem.* **2004**, *43*, 8218−8220.
(94) Collman, J. P.; Reed, C. A. *J. Am. Chem. Soc.* **1973**, *95*, 2048−2049.
(95) Ellison, M. K.; Schulz, C. E.; Scheidt, W. R. *Inorg. Chem.* **2002**, *41*, 2173−2181.
(96) Brault, D.; Rougee, M. *Biochem. Biophys. Res. Commun.* **1974**, *57*, 654−659.
(97) Rougee, M.; Brault, D. *Biochemistry* **1975**, *14*, 4100−4106.
(98) Wagner, G. C.; Kassner, R. J. *Biochim. Biophys. Acta* **1975**, *392*, 319−327.
(99) Collman, J. P.; Brauman, J. I.; Doxsee, K. M.; Halbert, T. R.; Suslick, K. S. *Proc. Natl. Acad. Sci. U.S.A.* **1978**, *75*, 564−568.

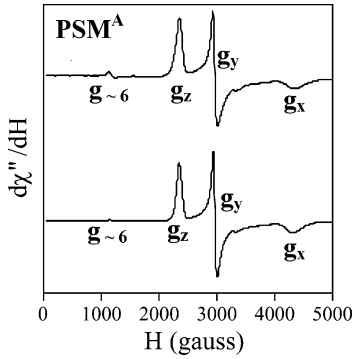

Figure 3. Frozen-solution X-band EPR spectra of PSM^A (top) and PSM^W (bottom), (approximately 0.5 mM) in a 50 mM phosphate buffer, pH 7.0, containing 20% (v/v) glycerol. Instrumental parameters: temperature, 20 K; microwaves, 2.0 mW at 9.5 GHz; modulation, 10 G at 100 kHz.

Supporting Information), indicating that the Ala to Trp replacement exerted little if any effect on porphyrin planarity.

The RR spectrum of Fe^{III}-$mPSM^A$ in 1:1 H_2O/MeOH features an oxidation-state marker band (ν_4) at 1372 cm^{-1} and a spin-state marker band (ν_3) at 1485 cm^{-1}. The corresponding bands in the RR spectrum of metMb,[103] which exhibits His−OH_2 ligation, occur at 1373 and 1483 cm^{-1}. The nearly identical frequencies of ν_3 and ν_4 for Fe^{III}-$mPSM^A$ and metMb indicate that the former is six-coordinate and, therefore, that water or methanol is ligated trans to the His ligand. The RR spectrum of $mPSM^A$ also features a weak band at 1506 cm^{-1}, closely matching the frequency of the ν_3 band in the RR spectrum of Fe^{III}-PSM^A. We interpreted this as indicating the presence of some six-coordinate low-spin Fe^{III} in $mPSM^A$ but argued that low-spin Fe^{III} accounts for only a minor fraction of the total Fe present.[28]

Electron Paramagnetic Resonance (EPR) Spectroscopy. EPR spectra of PSM^A and its isomers recorded at 11 K are similar to that of cyt b_5, with the three-line pattern expected for low-spin, rhombically distorted Fe^{III} and g values indicative of bis(His) ligation.[21,22,29] Rhombic distortion in ferric porphyrin bis(ImH) complexes provides strong evidence that the planes of the ligands are aligned approximately parallel to one another.[104] The planes of the imidazolyl groups in the PSMs are likely rotated relative to a given N−Fe−N axis in the porphyrin; an angle of ~20° is typical for bis(ImH) complexes of simple ferric porphyrins.[105] The g values observed for PSM^A ($g_x = 1.56$, $g_y = 2.30$, and $g_z = 2.87$) and PSM^W ($g_x = 1.57$, $g_y = 2.28$, and $g_z = 2.88$) are almost identical (Figure 3), indicating that the Ala to Trp replacement exerted little if any effect on His side-chain orientation. There is a small signal near $g = 6$ in each spectrum, which may be taken as evidence that a very small amount of high-spin Fe^{III} is present. However, the high-spin signal is more intense in the spectrum of PSM^A than in that of PSM^W, suggesting that the Ala to Trp replacement strengthened His−Fe ligation. This was confirmed in pH titration studies described in a subsequent section.

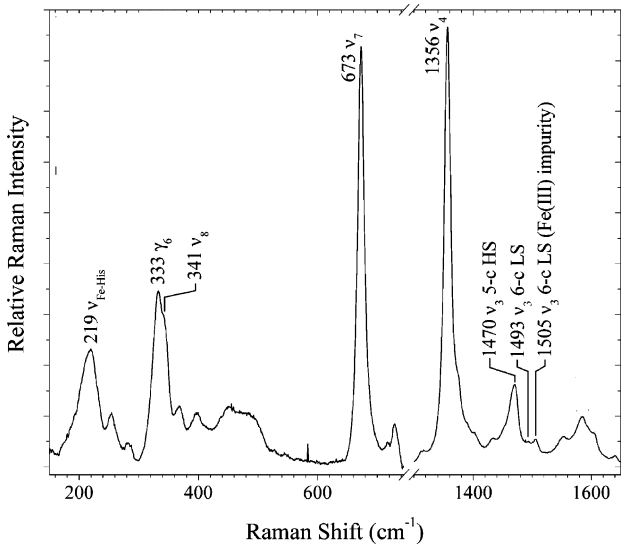

Figure 4. Low-frequency (180−740 cm^{-1}) and high-frequency (1300−1640 cm^{-1}) RR spectra of $mPSM^A$ obtained at pH 7 and 25 °C in 1:1 H_2O/CH_3OH with 406.7-nm excitation.

The EPR spectrum of Fe^{III}-$mPSM^A$, recorded at 11 K in a solvent that prevented aggregation, was dominated by signals with $g = 5.71$ and 1.98,[28] indicative of axially distorted Fe^{III} (Figure S4 in the Supporting Information). The position of the former signal indicates that Fe^{III} is predominantly high spin ($S = {}^5/_2$). We also observed evidence for a small amount of low-spin ($S = {}^1/_2$) Fe^{III} in thermal equilibrium with the $S = {}^5/_2$ form, supporting our interpretation of the RR data.

Fe^{II} State

Fe^{II}-$mPSM^A$. We begin our discussion of the ferrous state with $mPSM^A$. Reduction of Fe^{III} to Fe^{II} in $mPSM^A$ in a 60:40 H_2O/MeOH solution at pH 8 using sodium dithionite shifted its Soret band λ_{max} from 391 to 420 nm, and a broad band appeared near 550 nm in the visible region (Figure S1B in the Supporting Information; dashed line).[22,30] Sodium dithionite absorbs very strongly in the far-UV region, and it was therefore not possible to determine by CD whether reduction of Fe^{III}-$mPSM^A$ led to rupture of the His−Fe bond. However, lowering the pH from 8 to 6 in a solution of Fe^{II}-$mPSM^A$ resulted in the appearance of a shoulder on the Soret band near 406 nm, close to the Soret band λ_{max} of iron(II) coproporphyrin I in aqueous solution.[30] This strongly suggested that Fe^{II}-$mPSM^A$ is mono(His)-ligated at pH 8 but that the ligand begins to dissociate by pH 6. Figure 4 shows the previously unpublished RR spectra of Fe^{II}-$mPSM^A$. The high-frequency region of the spectrum exhibits a spin-state marker band (ν_4) at 1356 cm^{-1} and an oxidation-state marker band (ν_3) at 1470 cm^{-1}. The corresponding bands occur at nearly identical frequencies in RR spectra of deoxyHb ($\nu_4 = 1358$ cm^{-1}; $\nu_3 = 1472$ cm^{-1})[106] and Fe^{II}-MPIX(2-MeImH) ($\nu_4 = 1359$ cm^{-1}; $\nu_3 = 1472$ cm^{-1}),[107] both of which exhibit

(100) Choi, S.; Spiro, T. G. *J. Am. Chem. Soc.* **1983**, *105*, 3683−3692.
(101) Choi, S.; Spiro, T. G.; Langry, K. C.; Smith, K. M.; Budd, D. L.; La Mar, G. N. *J. Am. Chem. Soc.* **1982**, *104*, 4345−4351.
(102) Kitagawa, T.; Sugiyama, T.; Yamano, T. *Biochemistry* **1982**, *21*, 1680−1686.
(103) Hu, S.; Smith, K. M.; Spiro, T. G. *J. Am. Chem. Soc.* **1996**, *118*, 12638−12646.
(104) Walker, F. A.; Huynh, B. H.; Scheidt, W. R.; Osvath, S. R. *J. Am. Chem. Soc.* **1986**, *108*, 5288−5297.
(105) Scheidt, W. R.; Lee, Y. J. *Struct. Bonding (Berlin)* **1987**, *64*, 1−70.

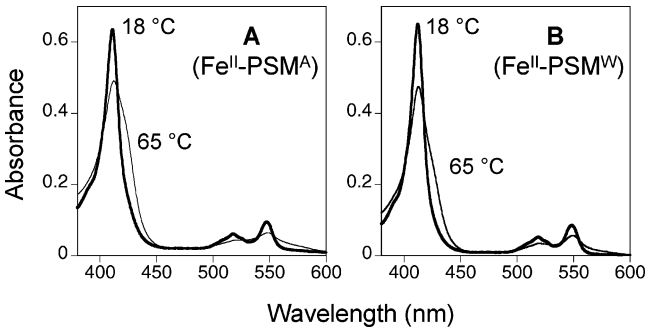

Figure 5. UV/vis spectra of Fe^{II}-PSM^A (A) and Fe^{II}-PSM^W (B) recorded between 18 °C (thin line) and 65 °C (bold line) in aqueous solution at pH 7.

five-coordinate Fe^{II}. The low-frequency region of the RR spectrum of Fe^{II}-$mPSM^A$ features a strong band centered at 219 cm^{-1}, which can be safely assigned as a His−Fe^{II} stretch. The Fe−His stretches in the spectra of Mb,[108] Hb,[109] and Fe^{II}PPIX(2-MeImH)[109] in aqueous solution appear at 220 cm^{-1}. On the basis of these observations, it can be concluded that Fe^{II}-$mPSM^A$ exhibits five-coordinate, mono(His)-ligated Fe.

Fe^{II}-PSM^A and Fe^{II}-PSM^W. Reduction of Fe^{III} to Fe^{II} in PSM^A and PSM^W at 8 °C led to spectra characteristic of low-spin Fe^{II} (Figure S1A in the Supporting Information; dashed line) as was expected for bis(His)-ligated iron(II) mesoporphyrin, with λ_{max} at 411 nm and distinct α/β bands in the visible region.[22] However, new bands matching those in the spectrum of Fe^{II}-$mPSM^A$ began to appear in the Fe^{II}-PSM^A and Fe^{II}-PSM^W spectra at higher temperatures, but at any given temperature, they were more prominent in the case of Fe^{II}-PSM^A (Figure 5).[22,30] It was therefore possible to conclude that the Fe^{II}-PSMs exist in equilibrium between low-spin ($S = 0$) bis(His)-ligated and high-spin ($S = 2$) mono(His)-ligated forms, with the former predominating.

Aromatic Side Chain−Porphyrin Interactions Stabilize the PSM Fold

Lowering the pH from 7 to 2 led to complete loss of the peptide helix content in all of the ferric PSMs and conversion of Fe^{III} from the low-spin state to the high-spin state, indicating dissociation of both His ligands.[21,22,26] We observed clean isosbestic behavior in pH titrations of the MPII variants of PSM^A and PSM^W performed in aqueous methanol solutions and were thus able to determine stepwise equilibrium constants for binding of the first (K_1^{III}) and second (K_2^{III}) His ligand in each compound.[29] The midpoint values in these pH titrations (pK_{app}) are defined in eq 1, where K_a is the acid dissociation constant for the protonated His side chain in the His-dissociated state. The K_a values for PSM^A and PSM^W were estimated from the acid dissociation constants of the His side chains in the individual peptide components in aqueous solution, determined by ^1H NMR. Table 1 reports the results of regression analysis of pH titration data for Fe^{III}-PSM^A performed in a 30% MeOH solution and for Fe^{III}-PSM^W in a 25% MeOH solution using an expanded form of eq 1 (eq S2 in the Supporting Information).[29] Also reported in Table 1 is the equilibrium constant (K_1^{III}) for the formation of a single His−Fe bond in Fe^{III}-$mPSM^A$ in a 40% MeOH solution.[28] In the case of Fe^{III}-$mPSM^A$, CD spectra exhibited much larger pH-dependent changes than did UV/vis spectra, and the CD data were therefore chosen for analysis. The inflection point in the titration ($pK_{app} = 3.83$) is defined in eq 2. Using the K_a value for His noted above, eq 2 shows that $K_1^{III} = 462$ ($\Delta G° = -3.7$ kcal/mol) for Fe^{III}-$mPSM^A$, comfortingly similar to the results obtained for PSM^A in a 30% MeOH solution.

$$pK_{app} = -\log[K_a(K_1^{III}\,K_2^{III})^{1/2}] \quad (1)$$

$$pK_{app} = pK_a + pK_1^{III} \quad (2)$$

The data in Table 1 show that K_2^{III} is about 6-fold (1 kcal/mol) larger than K_1^{III} in both PSM^A (Figure S5A in the Supporting Information) and PSM^W (Figure S5B in the Supporting Information), analogous to the situation for ImH binding by simple iron(III) porphyrins. K_1^{III} and K_2^{III} are both 8−9-fold ($\Delta\Delta G° = 1.2-1.3$ kcal/mol) larger for Fe^{III}-PSM^W than for Fe^{III}-PSM^A, however, which we attribute to the entropically favorable scattering of water molecules due to Trp side chain−porphyrin interactions (the hydrophobic

Table 1. Ligand Binding Data

compound	ligand	method	solvent	equilibrium constant	$\Delta G°$ (kcal/mol)	ref
Fe^{III}-$mPSM^A$	His	pH, CD	40% MeOH	$K_1^{III} = 462$	−3.7	28
Fe^{III}-PSM^A	His(1)	pH, spec.	30% MeOH	$K_1^{III} = 223$	−3.2	29
	His(2)	pH, spec.		$K_2^{III} = 1.45 \times 10^3$	−4.3	29
Fe^{II}-PSM^A	His(1)	pH, spec.	H_2O	$K_2^{II} = \sim 3$	~ -0.7	30
Fe^{III}-PSM^W	His(1)	pH, spec.	25% MeOH	$K_1^{III} = 2.02 \times 10^3$	−4.5	29
	His(2)	pH, spec.		$K_2^{III} = 1.21 \times 10^4$	−5.6	29
Fe^{II}-PSM^W	His(2)	pH, spec.	H_2O	$K_2^{II} \sim 9$	~ -1.3	30
Fe^{II}-PSM^A	CO	spec.	H_2O	$K_{CO}^{II} = 8.4 \times 10^7\ M^{-1}$	−10.9	30
	CO	pot.	H_2O	$K_{CO}^{II} = 3.0 \times 10^7\ M^{-1}$	−10.2	this work
	DMSO	spec.	H_2O	$K_{DMSO}^{II} = 8.9\ M^{-1}$	−1.3	this work
	DMSO	pot.	H_2O	$K_{DMSO}^{II} = 12.3\ M^{-1}$	−1.5	this work
Fe^{III}-$mPSM^A$	ImH	spec.	40% MeOH	$K_{ImH}^{III} = 7728\ M^{-1}$	−5.5	this work
Fe^{II}-$mPSM^A$	ImH	spec.	40% MeOH	$K_{ImH}^{II} = 169\ M^{-1}$	−3.0	this work
Fe^{III}-$mPSM^A$	DMSO	spec.	40% MeOH	$K_{DMSO}^{III} < 1\ M^{-1}$	>0	this work
Fe^{II}-$mPSM^A$	DMSO	spec.	40% MeOH	$K_{DMSO}^{II} = 177\ M^{-1}$	−3.1	this work

effect) with additional possible contributions from Trp/His π-stacking interactions (see Figure 1). Increasing hydrophobic peptide−porphyrin interactions in 2:1 complexes between His-containing peptides and water-soluble ferric porphyrins[78,110] or analogous 1:1 complexes involving hairpin peptides[77] have likewise been shown by the Suslick and Mihara laboratories to substantially increase stability.

Relative amounts of the low- and high-spin forms of Fe^{II}-PSM^A and Fe^{II}-PSM^W could be estimated from UV/vis data, using spectra of Fe^{II}-MPIX$(ImH)_2$ and of Fe^{II}-$mPSM^A$, respectively, as models.[30] The data in Table 1 show that the second His ligand is coordinated about 3-fold more strongly in Fe^{II}-PSM^W than in Fe^{II}-PSM^A.[30]

Helix Induction Weakens His−Fe Ligation in the PSMs

Spectrophotometric titrations of ImH with Fe^{II}-$mPSM^A$ (Figure S6 in the Supporting Information) and Fe^{III}-$mPSM^A$ (Figure S7 in the Supporting Information) were performed in 60:40 H_2O/MeOH at pH 8 and 25 °C (see Table 1). ImH was found to bind ~46-fold (2.5 kcal/mol) more strongly to Fe^{III}-$mPSM^A$ than to Fe^{II}-$mPSM^A$. In each case, a low-spin 1:1 complex was formed, indicating that the endogenous His ligand remained coordinated to Fe. The data in Table 1 show that binding of ImH to $mPSM^A$ is accompanied by a more negative free-energy change than is binding of the second His ligand in PSM^A. In other words, the peptide linkers in the PSMs *weaken* axial ligation relative to an exogenous ImH ligand. While this phenomenon took us by surprise at first, it is consistent with our strategy of utilizing His−Fe binding energy to overcome the unfavorable entropy of peptide helix induction. A very interesting observation from this study is that the peptide linkers lead to greater weakening of His−Fe^{II} ligation ($\Delta\Delta G° = 2.3$ kcal/mol) than of His−Fe^{III} ligation ($\Delta\Delta G° = 1.2$ kcal/mol).

2,2,2-Trifluoroethanol (TFE) Diminishes the Conformational and Stability Differences in PSM^A and PSM^W

Fe^{III}. Alcoholic solvents such as TFE and methanol are able to increase the helix content in a peptide, largely by reducing the concentration of hydrogen-bonding groups present in the medium. At 25 °C and pH 8, 25% TFE increases the helix content in PSM^A by nearly a factor of 2 but exerts a negligible effect on the helix content in PSM^W (Table 2). The data in Table 2 show that 25% TFE also stabilizes His−Fe^{III} ligation (as indicated by K_{app}) in Fe^{III}-PSM^A (12-fold) to a much greater extent than in Fe^{III}-PSM^W (2.5-fold). As a result, Fe^{III}-PSM^A and Fe^{III}-PSM^W are much more similar in terms of peptide conformation and stability in 25% TFE (Fe^{III}-PSM^A is approximately 2-fold more stable) than they are in aqueous solution (Fe^{III}-PSM^A is approximately 9-fold more stable). MeOH at 25 vol % also diminishes differences in the helix content and stability between these two PSMs, albeit to a smaller extent than was achieved by TFE.

Table 2. PSM Redox, CD, and Stability Data

	$E_{m,8}$ (mV vs SHE)			helix content (%)			10^4K_{app}[a]		
compound	H_2O	25% MeOH	25% TFE	H_2O	25% MeOH	25% TFE	H_2O	25% MeOH	25% TFE
PSM^A	−281	−314	−337	36	56	69	0.5	1.5	6.0
PSM^W	−337	−344	−349	74	83	78	4.4	7.9	11.0
FeMPIX-$(ImH)_2$[b]	−280	−284	−304	*c*	*c*	*c*	*d*	*d*	*d*

[a] From pH titrations. [b] Measured in the presence of 5 M ImH. [c] Not applicable. [d] Not determined.

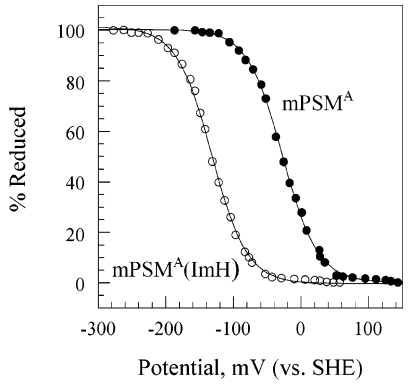

Figure 6. Redox potentiometry data monitored by UV/vis for $mPSM^A$ in the absence (●) and presence (○) of 100 mM ImH. Conditions: pH 8.0 and 25 °C in 60:40 H_2O/MeOH, 100 mM NaCl, and 50 mM Tris/HCl buffer. The curves were fitted to a strict $n = 1$ Nernst equation (solid lines).

Fe^{II}. By monitoring the intensity of the shoulder near 420 nm by UV/vis spectroscopy, we found that 25% TFE also stabilized His−Fe ligation in Fe^{II}-PSM^A to a greater extent than it did in Fe^{II}-PSM^W. In neither case, however, was the extent of stabilization as large as that observed for the corresponding Fe^{III}-PSMs. Thus, enhancing the helix content by use of TFE stabilizes His−Fe^{III} ligation to a greater extent than His−Fe^{II} ligation, analogous to the effect of introducing aromatic side-chain porphyrin interactions into PSM^A.

New Insight into Nature's Solutions for Tuning the Heme Protein Redox Potential

PSM^A vs $mPSM^A$(ImH). The $E_{m,8}$ value of $mPSM^A$ in 60:40 H_2O/MeOH is −24 mV, but the addition of 100 mM ImH (sufficient to achieve >95% saturation in both oxidation states) shifts it to −124 mV (Figure 6). The shift in the redox potential expected in such a system is described by eq 3, where L = ImH in this case. Upon incorporation of the K_{ImH}^{III}

$$\Delta E_m = (-RT/nF)\ln\{(1 + K_L^{III}[L])/(1 + K_L^{II}[L])\} \quad (3)$$

and K_{ImH}^{II} values determined in our equilibrium binding studies, eq 3 predicts that 100 mM ImH will result in $\Delta E_{m,8} = -98$ mV for $mPSM^A$ at 25 °C, remarkably similar to the observed effect.

Heme solvent exposure is the factor typically considered most important in tuning the redox potentials of heme

(106) Spiro, T. G.; Strekas, T. C. *J. Am. Chem. Soc.* **1974**, *96*, 338−345.
(107) Spiro, T. G.; Burke, J. M. *J. Am. Chem. Soc.* **1976**, *98*, 5482−5489.
(108) Argade, P. V.; Sassaroli, M.; Rousseau, D. L.; Inubushi, T.; Ikeda-Saito, M.; Lapidot, A. *J. Am. Chem. Soc.* **1984**, *106*, 6593−6596.
(109) Hori, H.; Kitagawa, T. *J. Am. Chem. Soc.* **1980**, *102*, 3608−3613.
(110) Huffman, D. L.; Suslick, K. S. *Inorg. Chem.* **2000**, *39*, 5418−5419.

proteins having identical axial ligation,[111−116] although differences in the axial ligand orientation[41] and basicity[40] can also play important roles. As noted previously, increasing the solvent exposure generally leads to negative shifts in the redox potential due to stabilization of Fe^{III} relative to Fe^{II}. It is, therefore, noteworthy that the $E_{m,8}$ value of $mPSM^A$(ImH) in 40% MeOH (−124 mV) is considerably more positive than that of PSM^A under similar solvent conditions (−314 mV in 30% MeOH), despite the fact that its porphyrin is much more solvent-exposed. Approximately 55 mV of the more positive $E_{m,8}$ value of $mPSM^A$(ImH) in comparison to PSM^A results from the greater weakening of Fe^{II} ligation ($\Delta\Delta G° = 2.3$ kcal/mol) than of Fe^{III} ligation ($\Delta\Delta G° = 1.2$ kcal/mol), resulting from replacement of the exogenous ImH ligand in $mPSM^A$(ImH) with the His-containing peptide in PSM^A. The remainder of the negative shift is clearly due to other sources, one of which may be the fact that "replacing" ImH with the His-containing peptide introduces three negatively charged Glu residues, which will tend to stabilize Fe^{III} relative to Fe^{II}.[117] Clearly, the rather substantial difference in solvent exposure between PSM^A and $mPSM^A$(ImH) is of little importance in governing their redox potentials. This highlights the danger of comparing the redox potentials of proteins exhibiting significant structural differences.

PSM^A vs PSM^W. We have summarized the results of studies indicating that Trp side chain−porphyrin interactions in PSM^W decrease the extent of contact between water and the porphyrin relative to PSM^A. We therefore predicted that $E_{m,8}$ of PSM^W would be more positive than that of PSM^A. We observed exactly the opposite, with PSM^W exhibiting an $E_{m,8}$ value 56 mV more negative than that of PSM^A in aqueous solution (Table 2).[29] In fact, PSM^W has the most negative redox potential in aqueous solution among currently known bis(His)-ligated heme protein mimetics.[7] The explanation for the more negative redox potential of PSM^W in comparison to PSM^A was provided by the results of our intramolecular ligand binding studies (Table 1) and, in fact, was the impetus behind those studies. Equation 4 relates the shift in the midpoint potential between two PSMs to differences in the stepwise ligand binding constants in the Fe^{III} and Fe^{II} states. In eq 4, $\beta_2^{III} = K_1^{III} K_2^{III}$ (for derivation of

$$\Delta\Delta E_m = (-RT/nF)\{\ln[\beta_2^{III}(PSM^A)/\beta_2^{III}(PSM^W)] - \ln[K_1^{II}(1 + K^{II})(PSM^A)]/[K_1^{II}(1 + K^{II})(PSM^W)]\} \quad (4)$$

eq 4, see the Supporting Information for ref 29). Using values of β_2^{III} determined in the pH titrations in aqueous methanol solutions described previously (extrapolated to purely aqueous conditions), K_2^{II} values estimated from UV/vis spectra, and the assumption that replacing Ala by Trp will affect K_1^{II} to the same extent that it affects K_2^{II}, eq 4 predicts a −90 mV shift on going from PSM^A to PSM^W.[29] Thus, replacing the two Ala-4 residues in PSM^A with Trp led to a negative shift in the redox potential predominantly because it stabilized His−Fe^{III} ligation (8−9-fold) to a significantly greater extent than His−Fe^{II} ligation (∼3-fold). The fact that the measured $\Delta E_{m,8}$ value (−58 mV) is less negative than the calculated value ($\Delta E_{m,8} = -90$ mV) suggests a possible contribution from the lower porphyrin solvent exposure in PSM^W than in PSM^A.

In studies that have not previously been published, we observed that $E_{m,8}$ of PSM^A was strongly affected by the presence of alcohol cosolvents (Table 2). It became 33 mV more negative when the solvent was changed from water to 25% MeOH and 56 mV more negative when water was replaced by 25% TFE. The negative shifts can be attributed to the fact that methanol and TFE stabilize His−Fe^{III} ligation to a greater extent than His−Fe^{II} ligation. The $E_{m,8}$ value of PSM^W is much less sensitive to solvent changes because TFE exerts only minor effects on its helix content and stability (Table 2). It is noteworthy that the $E_{m,8}$ value of the control compound $FeMPIX(ImH)_2$ is also largely insensitive to methanol and TFE. A key observation from this study is that the $E_{m,8}$ values of PSM^A and PSM^W are much more similar in 25% TFE ($\Delta E_{m,8} = -12$ mV) than in aqueous solution ($\Delta E_{m,8} = -56$ mV). We have aready noted (see Table 2) that Fe^{III}-PSM^A and Fe^{III}-PSM^W are also more similar in terms of their helix content and stability in 25% TFE than in aqueous solution at 25 °C and pH 8.

The observations in this section suggest that stability may be more important than solvent exposure in tuning the redox potentials of heme protein variants having identical heme ligation motifs and highly similar structures. Support for this hypothesis has been provided by studies of the microsomal (Mc) and outer mitochondrial membrane (OM) isoforms of cyt b_5, which are described in the following sections.

Test Case for a Relationship between Stability and the Redox Potential: Mc and Mitochondrial cyt b_5

The genes coding for Mc and OM b_5 in vertebrates[118,119] likely arose via duplication of an ancestral gene.[120] One isoform is targeted to the membrane of the endoplasmic reticulum (microsomal, or Mc b_5) and the other to the outer mitochondrial membrane (OM b_5). Collaborative studies between our group and the Rivera and Kuczera laboratories[121−125] have focused primarily on the soluble heme-binding domains of bovine Mc (bMc) b_5 and rat OM (rOM) b_5, which exhibit 63% amino acid sequence identity (82% sequence similarity) and share essentially identical folds (see Scheme 3). OM b_5 $Fe^{III/II}$ redox potentials are significantly more negative ($E^{0'}$

(111) Tezcan, F. A.; Winkler, J. R.; Gray, H. B. *J. Am. Chem. Soc.* **1998**, *120*, 13383−13388.
(112) Gunner, M. R.; Honig, B. *Proc. Natl. Acad. Sci. U.S.A.* **1991**, *88*, 9151−9155.
(113) Churg, A. K.; Warshel, A. *Biochemistry* **1986**, *25*, 1675−1681.
(114) Stellwagen, E. *Nature* **1978**, *275*, 73−74.
(115) Rivera, M.; Seetharaman, R.; Girdhar, D.; Wirtz, M.; Zhang, X.; Wang, X.; White, S. *Biochemistry* **1998**, *37*, 1485−1494.
(116) Battistuzzi, G.; Borsari, M.; Cowan, J. A.; Ranieri, A.; Sola, M. *J. Am. Chem. Soc.* **2002**, *124*, 5315−5324.
(117) Varadarajan, R.; Zewert, T. E.; Gray, H. B.; Boxer, S. G. *Science* **1989**, *243*, 69−72.
(118) Lederer, F.; Ghrir, R.; Guiard, B.; Cortial, S.; Ito, A. *Eur. J. Biochem.* **1983**, *132*, 95−102.
(119) Kuroda, R.; Ikenoue, T.; Honsho, M.; Tsujimoto, S.; Mitoma, J.; Ito, A. *J. Biol. Chem.* **1998**, *273*, 31097−31102.
(120) Guzov, V. M.; Houston, H. L.; Murataliev, M. B.; Walker, F. A.; Feyereisen, R. *J. Biol. Chem.* **1996**, *271*, 26637−26645.

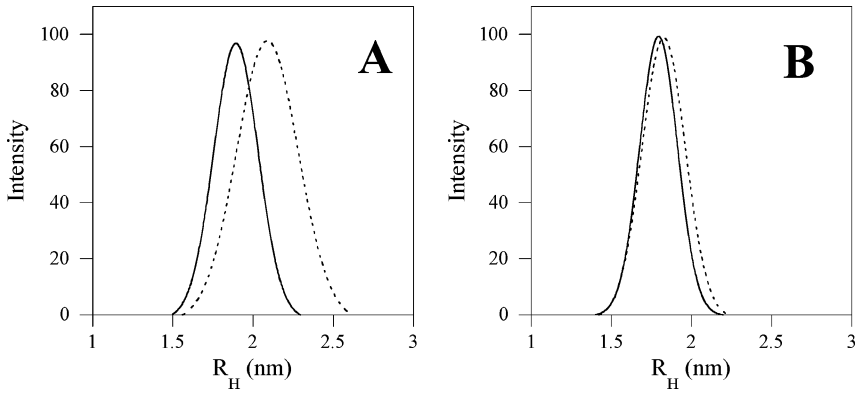

Figure 7. Size distribution plots comparing DLS data for the holo (solid lines) and apo (dashed lines) forms of (A) bMc b_5 and (B) rOM b_5. Data were recorded at 25 °C (pH 7.0; 50 mM potassium phosphate), with protein concentrations of 100 μM. The maxima in each plot represent the average hydrodynamic radius (size) of the protein, while the width of the band is a measure of its polydispersity (size distribution).

~ -70 mV for rOM b_5) than those of Mc b_5s ($E^{0'} \sim 0$ mV for bMc b_5),[122] but none of the factors normally invoked to explain differences in the redox potentials of two heme proteins with identical heme ligation appear to suffice in this case. Analysis of the X-ray crystal structures of bMc[63] and rOM b_5[126] has shown that their heme groups exhibit nearly identical solvent exposure[125] and electrostatic environments. Moreover, their His ligands reside in very similar hydrogen-bonding environments and have similar orientations.

As discussed above, PSM^W has a more negative redox potential than PSM^A despite having lower heme solvent exposure[29] and also differs from PSM^A in exhibiting greater stability[26,29] and lower peptide dynamic mobility[26] in aqueous solution. During the time period when we were making these discoveries, we determined that OM b_5's are considerably more stable than their Mc counterparts,[122,124] while molecular dynamics simulations[121,125] and HDX studies monitored by NMR[127] revealed lower polypeptide conformational mobility in OM b_5 than in Mc b_5. We have therefore proposed that the greater stability and lower dynamic mobility of OM b_5 in comparison to Mc b_5 are major contributors to the more negative OM b_5 redox potentials.[122,127,128] We believe that the results presented herein, showing that PSM^A and PSM^W $E_{m,8}$ values are nearly identical under conditions (25% TFE) that largely eliminate differences in stability and peptide conformation/dynamic mobility, provide strong support to this hypothesis.

In contrast to the holo proteins, Mc and OM apo-b_5 exhibit nearly identical thermodynamic stability at 25 °C and pH 7.[128] The greater stability of OM b_5's in comparison to Mc b_5's must therefore arise from stronger heme binding by its folded apoprotein. Studies of OM and Mc apo-b_5 in our laboratory have provided insight into how this might be achieved.[128−130] Removal of heme from Mc b_5 results in a 9.8% increase in the hydrodynamic radius (size), as determined by dynamic light scattering (DLS; Figure 7A),[128] due to disruption of the polypeptide conformation that is almost entirely limited to the heme binding pocket (core 1).[64,65] Removal of heme from rOM b_5 disrupts the core 1 polypeptide conformation to an extent virtually identical with that observed for bMc b_5 but results in only about a 3% expansion of the fold[128] (Figure 7B). The DLS data in Figure 7 also show that rOM apo-b_5 is less polydisperse than bMc apo-b_5, indicating that it populates a smaller number of disordered states. We have therefore proposed that OM apo-b_5 binds heme more strongly than Mc apo-b_5 because the reaction involves a smaller decrease in the non-native polypeptide conformational disorder, which is essentially a variation on the preorganization principle of Cram.[131]

Our studies have shown that factors tending to increase the overall stability of a PSM (cosolvents such as TFE, introduction of aromatic side chain−heme interactions, etc.) enhance His−Fe^{III} ligation to a significantly greater extent than His−Fe^{II} ligation, leading to negative redox potential shifts. It is therefore reasonable to propose that the stronger binding of heme by OM apo-b_5 than by Mc apo-b_5 might be greater in magnitude for ferric heme than for ferrous heme, providing another means by which the more negative redox potentials of the OM b_5's might be understood. It has unfortunately not proven possible to quantitate the difference in stability of the ferric and ferrous forms of OM and Mc b_5, but studies aimed at achieving that goal continue in our laboratories.

Why Does Reduction Reverse the Relative His Ligand Affinities in the PSMs?

The results of the intramolecular ligand binding studies show that reducing Fe^{III} to Fe^{II} in PSM^A and PSM^W reverses

(121) Altuve, A.; Silchenko, S.; Lee, K.-H.; Kuczera, K.; Terzyan, S.; Zhang, X.; Benson, D. R.; Rivera, M. *Biochemistry* **2001**, *40*, 9469−9483.
(122) Altuve, A.; Wang, L.; Benson, D. R.; Rivera, M. *Biochem. Biophys. Res. Commun.* **2004**, *314*, 602−609.
(123) Cowley, A. B.; Altuve, A.; Kuchment, O.; Terzyan, S.; Zhang, X.; Rivera, M.; Benson, D. R. *Biochemistry* **2002**, *41*, 11566−11581.
(124) Silchenko, S.; Sippel, M. L.; Kuchment, O.; Benson, D. R.; Mauk, A. G.; Altuve, A.; Rivera, M. *Biochem. Biophys. Res. Commun.* **2000**, *271*, 467−472.
(125) Lee, K.-H.; Kuczera, K. *Biopolymers* **2003**, *69*, 260−269.
(126) Rodriguez-Maranon, M. J.; Qiu, F.; Stark, R. E.; White, S. P.; Zhang, X.; Foundling, S. I.; Rodriguez, V.; Schilling, C. L., III; Bunce, R. A.; Rivera, M. *Biochemistry* **1996**, *35*, 16378−16390.
(127) Simeonov, M.; Altuve, A.; Massiah, M. A.; Wang, A.; Eastman, M. A.; Benson, D. R.; Rivera, M. *Biochemistry* **2005**, *44*, 9308−9319.
(128) Cowley, A. B.; Rivera, M.; Benson, D. R. *Protein Sci.* **2004**, *13*, 2316−2329.
(129) Cowley, A. B.; Sun, N.; Rivera, M.; Benson, D. R. *Biochemistry* **2005**, *44*, 14606−14615.
(130) Sun, N.; Wang, A.; Cowley, A. B.; Altuve, A.; Rivera, M.; Benson, D. R. *Protein Eng., Des. Sel.* **2005**, *18*, 571−579.
(131) Cram, D. J. *Angew. Chem., Int. Ed.* **1988**, *25*, 1039−1057.

Scheme 4. Demonstration of "Dynamic Strain" and How It Can Lead to Discrimination against a Second His Ligand Coordinating Trans to Another in an Iron(II) Porphyrin and Enable Binding of a Stronger Ligand

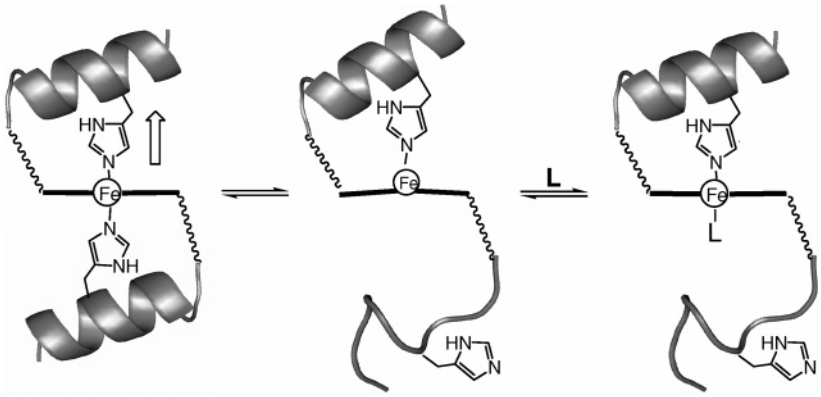

the relative affinities of the first and second His ligand for Fe ($K_2^{III} > K_1^{III}$ and $K_2^{II} < K_1^{II}$; Scheme 1). This is not typically the case in complexes between ImH and simple iron porphyrins[40,41] but is known to occur if strain is present as in complexes between 2-MeImH and ferrous porphyrins[94,95] and in T-Hb.[132] As was already noted, five-coordination in 2-MeImH−ferrous porphyrin complexes is due to a potential steric interaction that is relieved if Fe^{II} moves out of the mean porphyrin plane.[95] Traylor and co-workers referred to this steric interaction as face strain.[133] The out-of-plane motion has little effect on K_1^{II} but leads to virtually complete discrimination against binding of a second 1 equiv of 2-MeImH ($K_2^{II} \sim 0$; Scheme 1).[40,94,96] The use of sterically hindered ligands such as 2-MeImH with ferric porphyrins does not typically alter the relative order of binding constants observed with sterically undemanding analogues ($K_2^{III} > K_1^{III}$), although some exceptions have been reported.[134,135]

The out-of-plane Fe^{II} in T-Hb is not caused by face strain because the less hindered N_ϵ of His ligates to Fe in that protein. Rather, it is attributed to the protein's quaternary structure,[132,136] which places the proximal His ligands too distant from the heme centers to allow Fe^{II} to reside in the heme plane. Cooperative binding of four O_2 molecules relieves the tension, allowing the four Fe^{II} atoms to move back into the heme plane with the His ligands following, to give the relaxed (R) state.

The discrimination against binding of a second ligand in the Fe^{II}-PSMs is not as severe as it is in 2-MeImH complexes of ferrous porphyrins but suggests a phenomenon that causes Fe^{II} to periodically move in and out of the heme plane. Face strain is not likely in the PSMs because His probably ligates via N_ϵ in all cases, as is demonstrated by NMR for Co^{III}-PSM^A and Co^{III}-PSM^W.[26] It is also unrealistic to invoke a tense state for the PSMs because the peptides are simply too flexible to place a His ligand in a fixed location that disfavors an in-plane Fe^{II} location as occurs in T-Hb. One possible source of strain in at least some of the PSMs is unfavorable steric interactions between the peptide and porphyrin, perhaps near the point of covalent attachment.[22] Traylor and co-workers dubbed such a phenomenon spring-board strain.[133] We propose herein that a more important source of strain in the PSMs is simple dynamic fluctuation of the peptides, which occasionally pulls on one or the other His ligand, causing Fe^{II} to move out of plane (Scheme 4) and thereby weakening the bond to the other His ligand. Complete rupture of the bond to the second ligand can occur if Fe^{II} displacement is sufficiently large. We suggest the term "dynamic strain" to describe this phenomenon.

Six-Coordinate Ligand Binding Proteins

Several families of heme proteins have been discovered in which Fe has two protein-based axial ligands, one of which is displaced by a stronger gaseous ligand in the Fe^{II} state. For each example of such a "sensor" heme protein, there is an electron-transfer (ET) heme protein with identical ligation in the Fe^{II} state but which is inert to exchange with the same or even stronger ligands. The transcriptional regulator CooA from the bacterium *Rhodospirillum rubrum*[137] and the ET protein cytochrome f (a component of the cyt b_6f complex in chloroplasts[138]) represent an interesting example. The bis-(His)-ligated O_2 sensor neuroglobin and the ET protein cyt b_5 represent another.

CooA vs cyt f. Heme in Fe^{III}-CooA is ligated by one His side chain and by the thiolate side chain of a Cys residue,[139] but upon reduction to Fe^{II}-CooA, the Cys ligand is displaced by the protein N terminus, Pro-2 (Met-1 is removed following protein expression). If carbon monoxide (CO) is present, it displaces Pro-2 from Fe^{II}, triggering a conformational change that allows the protein to bind DNA and initiate transcription of the gene for CO dehydrogenase and for other proteins involved in CO oxidation. In contrast to CooA, cyt f exhibits

(132) Perutz, M. F.; Wilkinson, A. J.; Paoli, M.; Dodson, G. G. *Annu. Rev. Biophys. Biomol. Struct.* **1998**, *27*, 1−34.
(133) Geibel, J.; Cannon, J.; Campbell, D.; Traylor, T. G. *J. Am. Chem. Soc.* **1978**, *100*, 3575−3585.
(134) Ikezaki, A.; Nakamura, M. *Inorg. Chem.* **2002**, *41*, 6225−6236.
(135) Quinn, R.; Nappa, M.; Valentine, J. S. *J. Am. Chem. Soc.* **1982**, *104*, 2588−2595.
(136) Perutz, M. F. *Science* **1972**, *237*, 495−499.
(137) Roberts, G. P.; Kerby, R. L.; Youn, H.; Conrad, M. *J. Inorg. Biochem.* **2005**, *99*, 280.
(138) Kurisu, G.; Zhang, H.; Smith, J. L.; Cramer, W. A. *Science* **2003**, *302*, 1009−1014.
(139) Lanzilotta, W. N.; Schuller, D. J.; Thorsteinsson, M. V.; Kerby, R. L.; Roberts, G. P.; Poulos, T. L. *Nat. Struct. Biol.* **2000**, *7*, 876−880.

His−N_α ligation in both the Fe^{III} and Fe^{II} states and, to the best of our knowledge, is inert toward binding CO in the ferrous state.

Neuroglobin (Ngb) vs cyt b_5. Ngb is a member of a growing class of hexacoordinated hemoglobins (hxHbs), whose physiological roles are still a matter of debate. Like cyt b_5, Ngb exhibits bis(His) ligation in both the Fe^{III} and Fe^{II} states.[140] In contrast to cyt b_5,[141] however, Ngb binds both O_2 and CO in the Fe^{II} state.[142] Despite having six-coordinate heme Fe, the O_2 affinity of Ngb is similar to that of Mb.[143] Affinity of Ngb for O_2 appears to depend on the oxidative state of the cell: it has been shown to exist in both a high-affinity disulfide-containing form (with $K_{O_2} \sim 10^6$ M^{-1}) and a low-affinity form in which the disulfide bond is absent ($K_{O_2} \sim 10^5$ M^{-1}).[144] Even higher O_2 affinities ($K_{O_2} \sim 10^8$ M^{-1}) are exhibited by HxHbs from plants.[145]

PSMs as Models of Six-Coordinate Sensor Heme Proteins

The ability of Fe^{II} in CooA and Nb to bind their activating ligands provides clear evidence of a steady-state concentration of protein exhibiting five-coordinate Fe, as was observed for the Fe^{II}-PSMs.[146] This suggested to us that the PSMs might serve as useful models of six-coordinate sensor heme proteins. We relate herein studies of PSM^A with two competing ligands, one very weak and discovered accidentally (DMSO) and the other very strong (CO).

DMSO Binding by PSM^A. During preliminary redox potentiometry studies with PSM^A and PSM^W monitored by UV/vis spectroscopy, we noticed that the reduced compounds exhibited little evidence of the high-spin Fe^{II} form that is present following direct reduction with dithionite. Using $mPSM^A$, we determined that DMSO, the solvent used for stock solutions of the redox mediators, was responsible for this observation. DMSO (present at ~20 mM concentration in the redox studies) was competing with one of the His ligands in Fe^{II}-PSM^A for binding to Fe, giving a new low-spin complex. We subsequently replaced DMSO with dimethylformamide in mediator stock solutions. Spectrophotometric titrations revealed that DMSO is similar to ImH in its affinity for Fe^{II}-$mPSM^A$ (Table 1 and Figure S9 in the Supporting Information), and in studies with *N*-acetylmicroperoxidase-8 (a cyt *c* heme peptide), we have determined that it coordinates to Fe^{II} via O rather than S.[147] We have found DMSO to be an extremely poor ligand for Fe^{III}-$mPSM^A$ (Table 1 and Figure S10 in the Supporting Information) and, therefore, it cannot compete with His for binding to Fe in Fe^{III}-PSM^A. In the potentiometry studies, we were therefore observing a redox-mediated change in ligation from His−Fe^{III}−His to His−Fe^{II}−(O)DMSO (Scheme 4; L = DMSO). Because peptide helicity in the PSMs requires an intact His−Fe bond,[21,22] replacing His with DMSO is accompanied by a change in conformation from helix to coil, analogous in a fundamental sense to the effect of ligands on proteins such as CooA and Ngb. We performed a potentiometric titration of PSM^A in the presence of 200 mM DMSO (sufficient to achieve >95% saturation binding) and observed a 23-mV positive shift in the $E_{m,8}$ value (Figure 8**)**. When an exogenous ligand reacts with an iron porphyrin in the Fe^{II} state but not in the Fe^{III} state, the relationship between the binding constant and midpoint potential shift is described by eq 5 at the limit of high [L]. The equilibrium constant for DMSO binding by Fe^{II}-PSM^A determined via eq 5 is virtually identical with that determined in a spectrophotometric titration (Table 1 and Figure S8 in the Supporting Information). The data in Table 1 show that DMSO binds

$$\Delta E_m = (-RT/nF)\log(K_L^{II}[L]) \qquad (5)$$

about 10-fold (1.8 kcal/mol) more strongly to Fe^{II}-$mPSM^A$ than to Fe^{II}-PSM^A, but only 0.7 kcal/mol of the weaker binding by Fe^{II}-PSM^A can be directly attributed to the competing axial His ligand. The remaining ~1.1 kcal/mol likely arises from nonspecific (hydrophobic) interactions between the peptide and porphyrin in the His-dissociated form of Fe^{II}-PSM^A, which sterically blocks the ligand binding site.

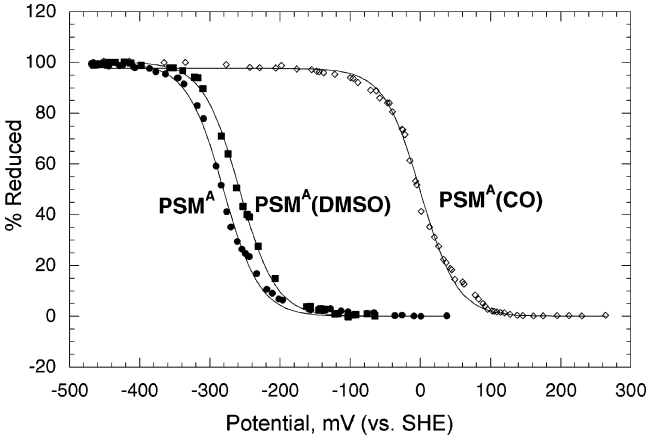

Figure 8. Redox potentiometry data monitored by UV/vis for PSM^A in aqueous solution and in the presence of saturating concentrations of DMSO (200 mM) and CO (840 μM). Conditions: pH 8.0 and 25 °C in 100 mM NaCl and a 50 mM Tris/HCl buffer. The curves were fitted to a strict $n = 1$ Nernst equation (solid lines).

CO Binding by PSM^A. The extremely negative redox potentials of the PSMs (vide infra) precluded binding studies with O_2, and they could therefore not be examined as models of Ngb. Fe^{II}-PSM^A does form a stable low-spin complex with CO, however (Scheme 4; L = CO).[30] Although near the limit of applicability of UV/vis spectroscopy for determining the strength of binding in such a system, we performed an

(140) Hankeln, T.; Ebner, B.; Fuchs, C.; Gerlach, F.; Haberkamp, M.; Laufs, T. L.; Roesner, A.; Schmidt, M.; Weich, B.; Wystub, S. *J. Inorg. Biochem.* **2005**, *99*, 110−119.
(141) Mathews, F. S.; Strittmatter, P. *J. Mol. Biol.* **1969**, *41*, 295−297.
(142) Trent, J. T., III; Watts, R. A.; Hargrove, M. S. *J. Biol. Chem.* **2001**, *276*, 30106−30110.
(143) Burmester, T.; Weich, B.; Reinhardt, S.; Hankeln, T. *Nature* **2000**, *407*, 461−462.
(144) Hamdane, D.; Kiger, L.; Dewilde, S.; Green, B. N.; Pesce, A.; Uzan, J.; Burmester, T.; Hankeln, T.; Bolognesi, M.; Moens, L.; Marden, M. C. *J. Biol. Chem.* **2003**, *278*, 51713−51721.
(145) Smagghe, B. J.; Sarath, G.; Ross, E.; Hilbert, J.-l.; Hargrove, M. S. *Biochemistry* **2006**, *45*, 561−570.
(146) Hargrove, M. S. *Biophys. J.* **2000**, *79*, 2733−2738.
(147) Lushington, G. R.; Cowley, A. B.; Silchenko, S.; Lukat-Rodgers, G. S.; Rodgers, K. R.; Benson, D. R. *Inorg. Chem.* **2003**, *42*, 7550−7559.

equilibrium binding study,[30] which yielded the data shown in Table 1. We have subsequently found that $E_{m,8}$ of PSM^A shifts from −283 to 0 mV at 24.4 °C in a saturated aqueous solution of CO (840 μM; Figure 8). Equilibrium constants and ligand binding free energies for CO determined via eq 5 are strikingly similar to those obtained via the equilibrium titrations (Table 1). It is noteworthy that the affinity for CO exhibited by PSM^A (3×10^7 M^{-1}) is toward the high end of the range of O_2 affinities reported for hxHbs (10^5-10^8 M^{-1})[144,145] and the CO affinity exhibited by CooA ($\sim 10^5$).[148]

Insight into Six-Coordinate Sensor Protein Function from Studies of the PSMs

Flexibility May Distinguish Sensor Heme Proteins from ET Heme Proteins with the Same Ligands. In CooA, Ngb, and the PSM examples described above, an endogenous nitrogenous ligand is being replaced by a stronger exogenous ligand and some of the ligand binding energy is invested in driving a structural change. In the PSMs, the change is very simple (helix to coil), but in the sensor proteins, the conformational change enables a "hidden" function or perhaps sends a signal. Geibel et al. were the first to discover that if two ImH moieties are covalently attached to an iron(II) porphyrin, the molecule exists in equilibrium between low-spin biscoordinated and high-spin monocoordinated states,[149] but at that time, no six-coordinate sensor heme proteins had been discovered. Geibel et al. instead used their observation to demonstrate that a rigid heme binding pocket was not necessary to enforce five-coordinate Fe^{II} in Hb and Mb. Gibney et al. showed that even in bis(His)-ligated heme protein maquettes, which are more protein-like than the PSMs, CO can effectively compete with one of the two axial His ligands for binding to Fe^{II}.[88] We have interpreted the results of our studies and those of Geibel et al. and Gibney et al. to indicate that six-coordinate sensor heme proteins take advantage of a fundamental property of heme: the much greater ease with which Fe^{II} rather than Fe^{III} can be pulled from the porphyrin plane, which is generally attributed to its larger ionic radius. The out-of-plane Fe^{II} displacement weakens the bond to the other ligand, lowering the activation barrier for its dissociation and thereby allowing the stronger exogenous ligand to bind.

We suggest that the greater tendency for Fe to move out of the plane in the Fe^{II}-PSMs than in simple complexes between ImH and iron(II) porphyrins is due to dynamic strain and tentatively propose that this mechanism may be operative in six-coordinate sensor heme proteins such as Ngb and CooA. All that is needed is a heme environment that allows for polypeptide conformational flexibility, particularly in the vicinity of the axial ligands. It is therefore interesting that X-ray crystallographic studies of Ngb have revealed (1) significant conformational flexibility of the polypeptide in contact with the prosthetic group, (2) the presence of cavities that allow the displaceable His ligand to move away,[150] and (3) that CO binding is accompanied by a "sliding" motion of the heme, which increases polypeptide structural order.[151] Perhaps, as suggested by Geibel et al.,[149] cyt b_5 cannot bind CO because it has "a more rigid heme environment which prevents the sixth (imidazole) ligand from leaving the iron". At the very least, rebinding of a dissociated intramolecular ligand in a typical ET heme protein such as cyt b_5 must be much faster than binding of a stronger exogenous ligand.

Ligand Concentration May Partially Govern Sensor Protein Reduction. Like the PSMs, the ferric forms of CooA ($E^{0'} = -300$ mV[152]) and Nb ($E^{0'} = -130$ mV[153]) are more stable than the ferrous forms under normal physiological conditions, and therefore they must be reduced prior to being able to bind their activating ligands. As suggested by Aono for CooA,[154] it may be advantageous for a sensor protein to be "stored" in a ferric form that is inert to the activating ligand and is also more stable than the ferrous form with respect to the conformational change that initiates its function. It has been shown that CO dehydrogenase only functions at redox potentials below −300 mV,[155] which has been taken to indicate that Fe^{III}-CooA is only reduced to the active ferrous form when the solution potential in the cell is <-300 mV (i.e., that CooA also functions as a redox sensor[137]). Our potentiometric ligand binding studies with PSM^A highlight another factor that may contribute to the reduction of Fe^{III}-CooA. Specifically, the equilibrium reduction potential of the protein becomes more positive (Fe^{III} becomes easier to reduce) as the CO concentration is increased. This occurs because binding of CO to the ferrous form of the protein stabilizes it relative to the ferric form. Thus, reduction of the ferric forms of CooA and other sensor heme proteins to the ferrous state may also be governed to some extent by the local concentration of the activating ligand.

Concluding Remarks

On the Design of His-Ligated, Helical Heme Proteins. Research with the PSMs was the first to show that ligation between a His ligand and heme Fe in a covalent heme peptide could induce helical conformations in short peptides in aqueous solution. In new results presented herein, we have shown that some of the His−Fe binding energy is invested in overcoming the unfavorable entropy change associated with helix induction, consistent with our design strategy. Furthermore, we have shown that the introduction of aromatic side chain−porphyrin hydrophobic interactions provides energy via the hydrophobic effect that is invested in two

(148) Yamashita, T.; Hoashi, Y.; Watanabe, K.; Tomisugi, Y.; Ishikawa, Y.; Uno, T. *J. Biol. Chem.* **2004**, *279*, 21394−21400.
(149) Geibel, J.; Chang, C. K.; Traylor, T. G. *J. Am. Chem. Soc.* **1975**, *97*, 5924−5926.
(150) Vallone, B.; Nienhaus, K.; Brunori, M.; Nienhaus, G. U. *Proteins: Struct., Funct., Bioinf.* **2004**, *56*, 85−92.
(151) Vallone, B.; Nienhaus, K.; Matthes, A.; Brunori, M.; Nienhaus, G. U. *Proc. Natl. Acad. Sci. U.S.A.* **2004**, *101*, 17351−17356.
(152) Nakajima, H.; Honma, Y.; Tawara, T.; Kato, T.; Park, S.-Y.; Miyatake, H.; Shiro, Y.; Aono, S. *J. Biol. Chem.* **2001**, *276*, 7055−7061.
(153) Dewilde, S.; Kiger, L.; Burmester, T.; Hankeln, T.; Baudin-Creuza, V.; Aerts, T.; Marden, M. C.; Caubergs, R.; Moens, L. *J. Biol. Chem.* **2001**, *276*, 38949−38955.
(154) Aono, S. *Acc. Chem. Res.* **2003**, *36*, 825−831.
(155) Heo, J.; Halbleib, C. M.; Ludden, P. W. *Proc. Natl. Acad. Sci. U.S.A.* **2001**, *98*, 7690−7693.

ways: (1) enhancing the helix content and (2) increasing the stability of the His-ligated state.

On the Relationship between the Heme Protein Structure and Redox Potential. It is extremely tempting to interpret or predict differences in the redox potential between heme protein variants solely on the basis of their three-dimensional structures. As most researchers interested in the relationship between the heme protein structure and redox potential are aware, it is not at all uncommon for predictions as to the direction or magnitude of a redox potential shift resulting from a site-directed mutation to be well off the mark. The structurally simple species $mPSM^{A}$(ImH), PSM^{A}, and PSM^{W} described herein highlight this problem very well: their redox potentials in aqueous solution cover quite a wide range (213 mV) but lie in an order precisely the opposite of what would be expected utilizing the common assumption that heme solvent exposure is the dominant factor when ligation does not change. Perhaps the most important finding in our redox studies is that changes in the structure of a bis(His)-ligated heme protein mimetic such as a PSM, or in conditions that lead to an increase in its stability, strengthen His−Fe^{III} ligation to a greater extent than His−Fe^{II} ligation. This can lead to a negative shift in the redox potential, even when the change decreases heme solvent exposure. Our studies with Mc and OM b_5, considered in light of our PSM studies, suggest that the greater sensitivity of Fe^{III}−His ligation than of Fe^{II}−His ligation to differences in holoprotein stability and dynamics and/or apoprotein preorganization may be one of the important factors governing the redox potential in natural heme proteins having identical heme ligation motifs.

On the Challenge of Recapitulating the Heme Ligation Properties of ET Proteins. Studies of heme protein mimetics performed in water often neglect the Fe^{II} state in favor of the typically more air-stable Fe^{III} oxidation state. If a ferric bis(His)-ligated heme protein mimetic exhibits coordination chemistry similar to that of cyt b_5, one might make the erroneous assumption that the Fe^{II} state does as well. Our studies with the PSMs have clearly shown that this is not always the case, and we therefore urge other researchers to give equal attention to the ferrous and ferric forms of heme protein mimetics.

We found that reduction of Fe^{III} to Fe^{II} in the PSMs results in an overall decrease in the His−Fe ligation strength, whereas the corresponding change in the redox state of b_5 and other heme proteins almost invariably strengthens heme binding. In addition, the Fe^{II}-PSMs exist in equilibrium between low-spin bis(His)-ligated and high-spin mono(His)-ligated states, whereas cyt b_5 remains strongly six-coordinate in both the Fe^{III} and Fe^{II} oxidation states. Thus, the PSMs are better analogues of six-coordinate sensor heme proteins than of cyt b_5. We hope that continuing efforts in our laboratory can help elucidate the structural factors that allow ET heme proteins to circumvent the inherent ease with which Fe^{II} is displaced from the heme plane, thereby allowing dissociation of one of the ligands.

Acknowledgment. D.R.B. acknowledges the American Heart Association, Heartland Affiliate (Grant 0151412Z), and the Petroleum Research Fund (37709-AC3) for supporting the work with heme protein mimetics and the National Science Foundation (Grant MCB-0446326) for their support of the cyt b_5 studies. K.R.R. acknowledges USDA (Grant 2001-35318-11204) and the Hermann Frasch Foundation (Grant 446-HF97).

Supporting Information Available: Experimental section, spectroscopic data, and data from binding and pH titrations. This material is available free of charge via the Internet at http://pubs.acs.org.

IC052205K